

AD

SSM
192

MIPR No. 73-589
AMCMS CODE: 691000.22.63516
HDL Proj: E053E3

HDL-TR-1637

SIMULATION OF A SIMPLE LORENTZ PLASMA
WITH A RANDOM DISTRIBUTION OF
INDUCTIVELY LOADED DIPOLES

by

George Merkel

CLEARED
FOR PUBLIC RELEASE

PLIPA 5/15/77

November 1973

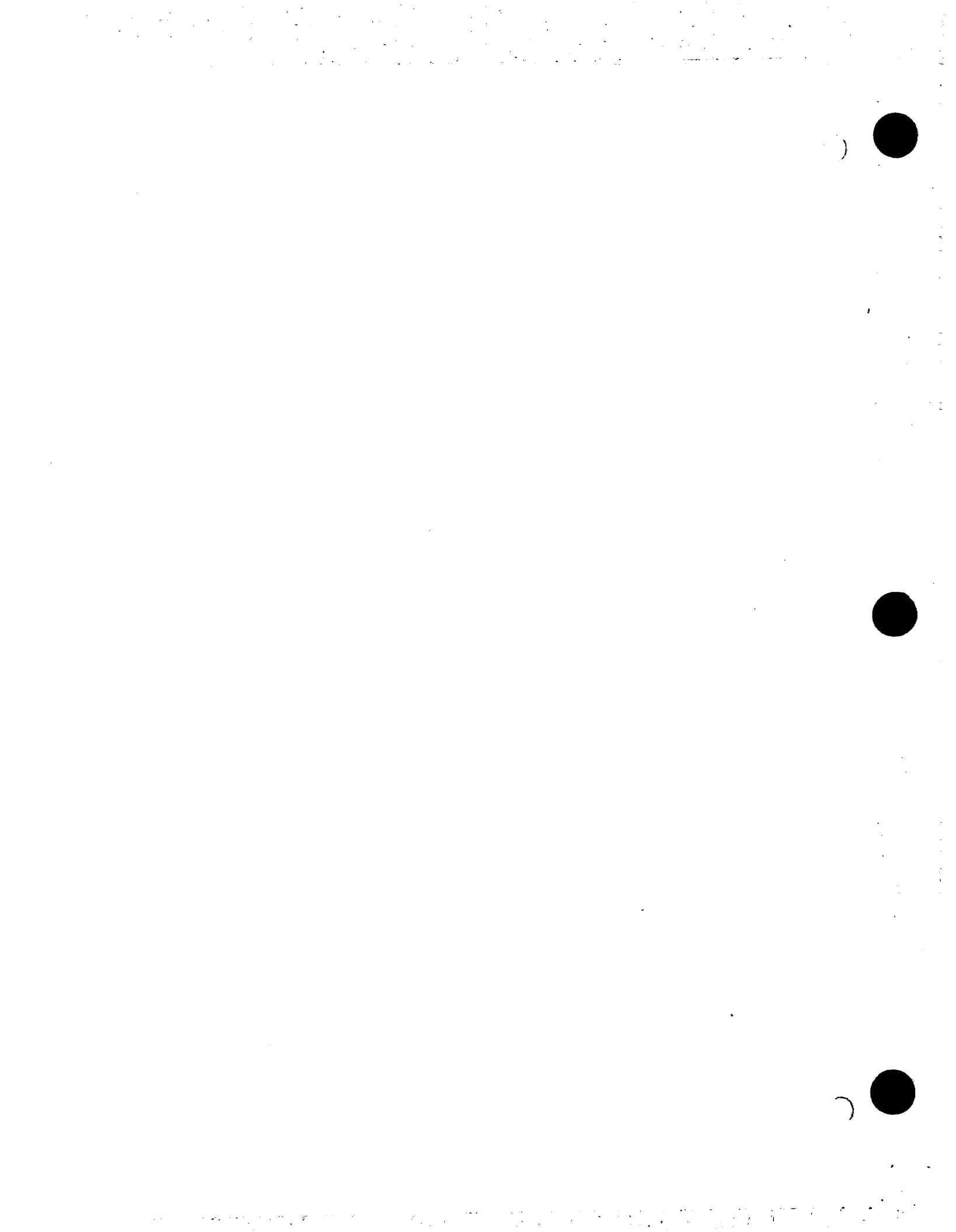
This research was sponsored by the Defense Nuclear Agency under
Subtask R99QAXEB088, Work Unit 04, "Source-Region Coupling."



U.S. ARMY MATERIEL COMMAND
HARRY DIAMOND LABORATORIES
WASHINGTON, D.C. 20438

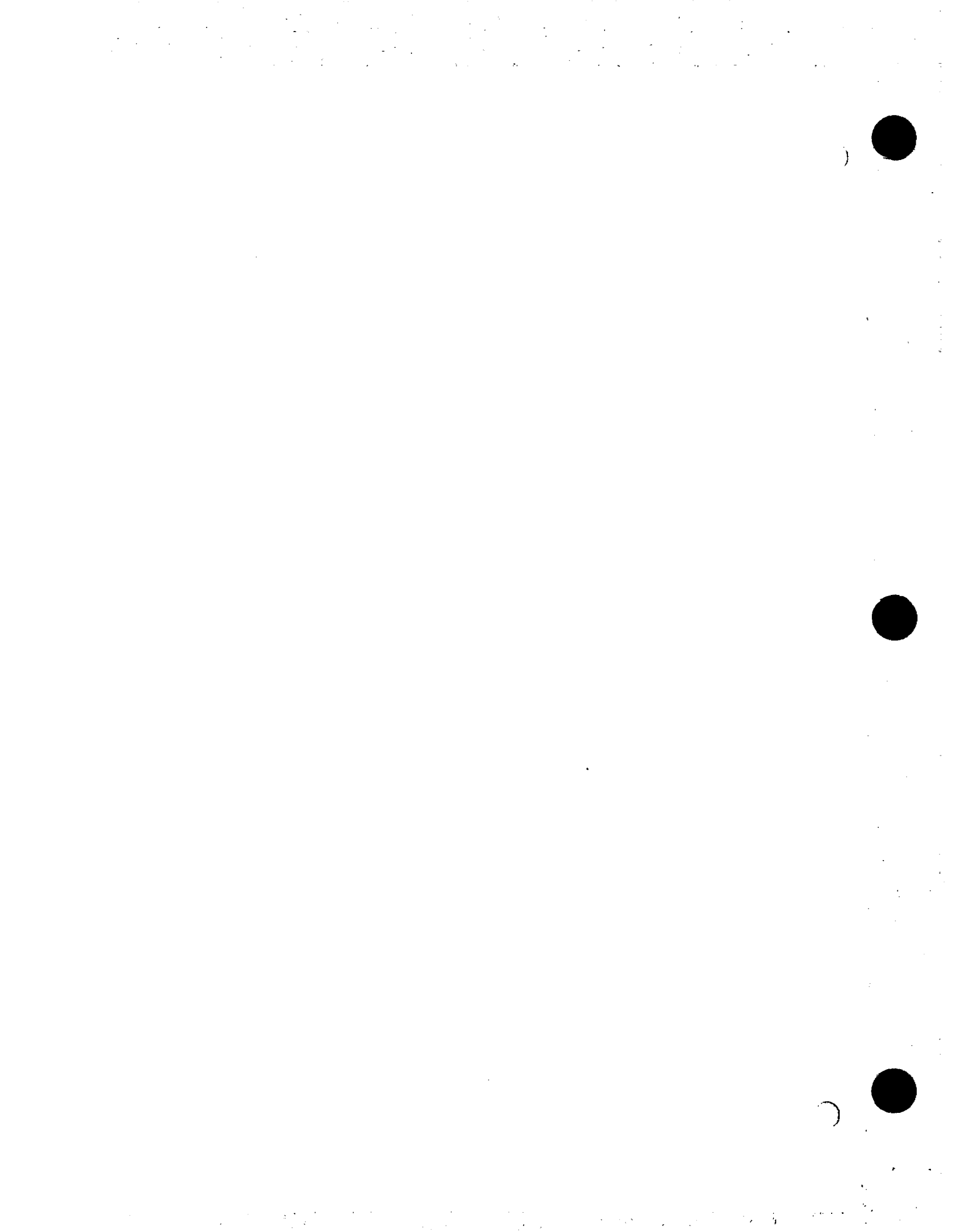
APPROVED FOR PUBLIC RELEASE; DISTRIBUTION UNLIMITED.

PL 96-1239



ABSTRACT

The feasibility of simulating a simple Lorentz plasma with an artificial dielectric constructed from a random distribution of inductively loaded dipoles is investigated. Both the differences and similarities between the macroscopic electromagnetic properties of the artificial dielectric and a Lorentz plasma are discussed.



FOREWORD

The work reported herein was sponsored by the Defense Nuclear Agency under Subtask EB-088 and by the In-House Laboratory Independent Research Program. We wish to thank Mr. Edward Greisch for obtaining the experimental data discussed in this report. We would also like to thank Mr. John Dietz for his many helpful suggestions.



CONTENTS

ABSTRACT	3
FOREWORD	5
1. INTRODUCTION	9
2. THEORETICAL DISCUSSION	11
2.1 Quasi-Static Approach	11
2.2 Explicit Consideration of Dipole Capacitance.....	16
2.3 Mutually Perpendicular Dipole Scatterers	20
2.4 Coupling of Scatterers	24
2.5 Deviations from the Clausius-Mossotti Equation Due to Randomness of Scatterers	31
3. COMPARISON OF EXPERIMENT WITH THEORY	34
4. SUMMARY AND CONCLUSIONS.....	42
REFERENCES	43
DISTRIBUTION	45
<u>FIGURES</u>	
1. Inductively loaded dipole	10
2. Lossless inductively loaded dipole.....	13
3. Two dipoles oriented in the θ and $-\theta$ directions	14
4. Two short dipole antennas	17
5. Two perpendicular inductively-loaded dipoles do not interact	22
6. The vector $p_{1,E1}$ is the dipole moment component of dipole 1 that is parallel to the incident electric field ...	23
7. The dipole moment of dipole 2 can be resolved into components parallel and perpendicular to the incident electric field	24
8. The vector $p_{1,E1}$ is the dipole moment component of dipole 1 that is perpendicular to the incident field	25
9. Spherical cavity in dielectric	26

FIGURES

10. Three-dimensional array of inductively-loaded dipoles enclosed in styrofoam spheres..... 29

11. Values of relative permittivity calculated with equations (36) and (42) for a number of different inductive loads. The other parameters are discussed in the text 35

12a. The real component of relative permittivity calculated with equations (69) and (42). The value used for L is .4 μ H and the value used for R is 0 Ω . The other parameters are the same as those employed to obtain figure 11 36

12b. The real component of relative permittivity calculates with equations (69) and (42). The value used for L is .4 μ H and the value used for R is 50 Ω . The other parameters are the same as those employed to obtain figure 11 37

12c. The real component of relative permittivity calculated with equations (69) and (42). The value used for L is .4 μ H and the value used for R is 100 Ω . The other parameters are the same as those employed to obtain figure 11 38

12d. The real component of relative permittivity calculated with equations (69) and (42). The value used for L is .4 μ H and the value used for R is 200 Ω . The other parameters are the same as those employed to obtain figure 11..... 38

13. Experimental setup used in determining the resonance frequency of the artificial dielectric. The sample consisted of 48 scatterers or "molecules." The V.S.W.R. or voltage standing-wave ratio was determined with a slotted line 39

14. Experimental standing-wave ratio corresponding to the setup shown in figure 13 39

15. The accuracy of the experimental points is limited by the granularity of the sample and the corresponding indefiniteness of the sample edges..... 41

1. INTRODUCTION

The complete simulation of the electromagnetic pulse, EMP, associated with a nuclear burst involves a number of interrelated parameters. The most obvious parameters are the waveform and the magnitude of the EMP. However, if the system being subjected to the nuclear EMP is in a pre-ionized region such as the ionosphere, we would also have to simulate the ionization or dielectric constant of the medium surrounding the system such as a missile or satellite. In this work we investigate the feasibility of using an artificial dielectric consisting of a random distribution of inductively loaded short dipoles to simulate the macroscopic electromagnetic properties of a simple Lorentz plasma.^{1,2}

During the past twenty-five years a number of so-called artificial dielectrics consisting of regularly spaced rods, parallel plates, metal spheres, etc. have been devised to reproduce the essential macroscopic properties of a dielectric. The ordinary artificial dielectric consists of discrete metallic or dielectric particles or lattices of macroscopic size.³⁻⁷ These artificial dielectrics were first actually conceived as large-scale macroscopic models of microscopic crystal lattices. The practical motivation for the development of the first artificial dielectrics was the desire to obtain relatively inexpensive lightweight materials that could be used for microwave and radar lenses. Several of the artificial dielectrics proposed for microwave lenses have the macroscopic electromagnetic properties of a plasma.^{2,4,8,9,10}

A review of the literature reveals a number of papers on the plasma simulation properties of artificial dielectrics consisting of a rigid cubic lattice of three-dimensional grids.^{2,4,8} Experimental work, reported in the literature, has been done only on two-dimensional grid lattice structures.^{2,8,10} That a periodic grid structure would produce band structure resonances analogous to Bragg scattering has been discussed from a theoretical viewpoint, but has not been experimentally investigated.^{11,12,13,14}

The rigid cubic grid lattice structure has the disadvantage of being somewhat unwieldy and difficult to support and fit around an object with curved surfaces. In general, the cubic lattice grid structure lends itself conveniently to simulation of flat, slab-like plasma sheaths.

In this paper we describe another approach to the simulation of a Lorentzian plasma. We propose a granular pellet-like artificial dielectric consisting of a random distribution of styrofoam spheres containing inductively loaded dipoles which can yield macroscopic electromagnetic constitutive relationships similar to those of a plasma.

A Lorentz plasma can be represented from the viewpoint of macroscopic electromagnetic theory, as a lossy dielectric with a complex dielectric constant given by^{1,2}

$$\epsilon_p = \epsilon_0 \left[1 - \frac{\omega_p^2}{\nu^2 + \omega^2} + j \frac{\omega_p^2 (\nu/\omega)}{(\nu^2 + \omega^2)} \right], \quad (1)$$

where ϵ_0 is the dielectric constant of free space, ω is the frequency of the electromagnetic field, ω_p is the plasma frequency, and ν is the collision frequency between electrons and the gas molecules. We propose to simulate this macroscopic dielectric constant with an artificial dielectric consisting of a random distribution of inductively loaded dipoles encased in styrofoam pellets. A schematic drawing of such a dipole is shown in figure 1. The quantities 2ℓ , L , and R are the length, inductance, and resistance of the loaded dipole respectively. As we will show, using simple quasi-static arguments, if the effective inductance ωL is much greater than the effective capacitance of the dipole, the permittivity of a random distribution of inductively loaded dipoles is

$$\epsilon_p = \epsilon_0 \left(1 - \frac{\frac{4}{3} \frac{\ell^2}{\epsilon_0} \frac{N}{L}}{\left(\frac{R}{L}\right)^2 + \omega^2} + j \frac{\frac{4}{3} \frac{\ell^2}{\epsilon_0} \frac{N}{L} \left(\frac{R}{L}\right) \frac{1}{\omega}}{\left(\frac{R}{L}\right)^2 + \omega^2} \right) \quad (2)$$

where N is the number density of the dipole pellets. One can see by comparing equation (1) with equation (2), that we can simulate a plasma with plasma frequency ω_p and collision frequency ν by setting

$$\frac{4}{3} \frac{\ell^2}{\epsilon_0} \frac{N}{L} = \omega_p^2 \quad (3)$$

and

$$\frac{R}{L} = \nu. \quad (4)$$

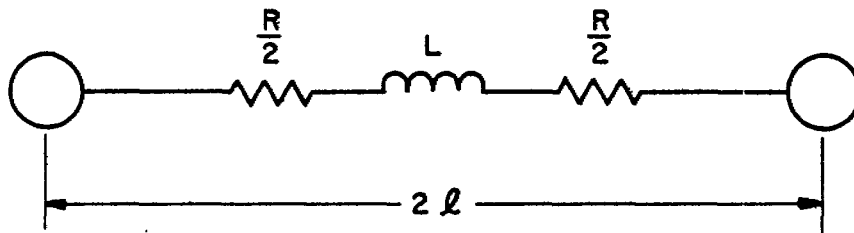


Figure 1. Inductively loaded dipole.

2. THEORETICAL DISCUSSION

2.1 Quasi-Static Approach

We will first approach the problem of our proposed artificial dielectric from a quasi-static viewpoint assuming that the inductive load of the dipole is much larger than the driving point capacitive impedance of a short dipole. In a subsequent section we will explicitly consider the dipole capacitance. First, we discuss the simulation of a tenuous plasma in which the collision frequency between free electrons and molecules, ν , is negligible.

We want to construct an artificial dielectric from a pellet-like medium that has an index of refraction given by²

$$n = (1 - \omega_p^2/\omega^2)^{1/2} \quad (5)$$

and an intrinsic impedance given by

$$\eta = \left(\frac{\mu_0}{\epsilon_p} \right)^{1/2} \quad (6)$$

where ϵ_p has a frequency dependence of the form^{1,2}

$$\epsilon_p = \epsilon_0 (1 - \omega_p^2/\omega^2) \quad (7)$$

and where ω_p is the plasma frequency.

In general the index of refraction of an artificial dielectric may be calculated in a manner analogous to that employed in calculating the index of refraction of a molecular medium. Assuming that the random obstacles are not too closely packed so that we do not have to resort to the Clausius-Mossotti relation, the index of refraction is given by⁵

$$n = \left[\epsilon_1 (1 + N\chi_e/\epsilon_0) \mu_1 (1 + N\chi_m/\mu_0) \right]^{1/2} \quad (8)$$

where

- N = Number of scattering obstacles per unit volume,
- χ_e = Electric polarizability of a scattering obstacle,
- χ_m = Magnetic polarizability of a scattering obstacle,
- ϵ_1 = 1 (for styrofoam),
- μ_1 = 1 (for styrofoam),

ϵ_0 = permittivity of free space,

μ_0 = permeability of free space.

From equations (5) and (8) we see that in order to achieve our goal we need an artificial dielectric constructed from obstacles that have a negative electric polarizability, χ_e . If the artificial dielectric is to simulate a plasma over a spectrum of frequencies, the value of χ_e must also be inversely proportional to the frequency squared. We would also like the value of the magnetic polarizability of the embedded obstacles, χ_m , to be : all or, if possible, zero.

A promising candidate for a scattering obstacle is an inductively loaded electric dipole. Consider the very idealized inductively loaded dipole schematically shown in figure 2. Let an electric field E be applied parallel to the line between two spheres separated by the distance 2ℓ . The field E then establishes a voltage $V=2\ell E e^{j\omega t}$ between the spheres. Assume that inductance between the two spheres is L , and also assume that $L\omega \gg 1/\omega C$ where C is the capacitance between the two spheres. Since we are dealing with a time harmonic field assume that the charge accumulated on the dipole spheres is given by

$$q = Qe^{j\omega t} \quad (9)$$

then

$$\begin{aligned} 2\ell E e^{j\omega t} &= L \frac{d^2q}{dt^2} \\ &= LQ(-\omega^2)e^{j\omega t} \end{aligned}$$

such that

$$Q = -2\ell E/L\omega^2$$

or

$$q = -2\ell E e^{j\omega t}/L\omega^2. \quad (10)$$

The dipole moment of the inductive dipole in figure 2 is then

$$p = 2\ell q = -4\ell^2 E e^{j\omega t}/L\omega^2$$

or

$$p = \chi_e E e^{j\omega t} \quad (11)$$

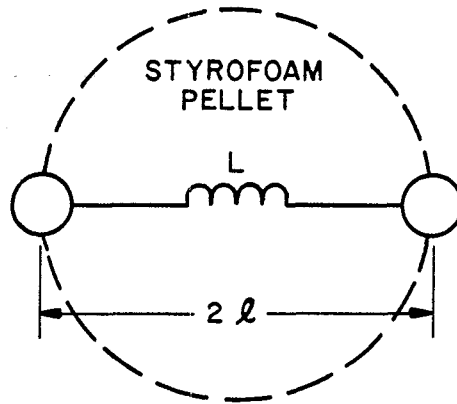


Figure 2. Lossless inductively loaded dipole.
The lossless dipole corresponds to a collisionless plasma.

where

$$\chi_e = -4\ell^2/L\omega^2. \quad (12)$$

If we have a random distribution of dipoles, we must, naturally, consider the various orientations that the dipoles can assume. As shown in figure 3 let the E field be in the Z direction. For every random dipole direction θ , we have an equally probable direction $-\theta$. We can therefore pair all the dipoles oriented in the $+\theta$ direction with dipoles oriented in the $-\theta$ direction. The resultant effective dipole moment for a dipole is

$$p(\theta) = -2 \cos \theta (\ell 2\ell \cos \theta) E e^{j\omega t}/L\omega^2.$$

The average value for a random distribution of directions, p_{av} , is then

$$\begin{aligned} p_{av} &= \int_0^{\pi/2} -4 \cos^2 \theta (\ell^2 E e^{j\omega t}/L\omega^2) 2\pi \sin \theta d\theta / 2 \int_0^{\pi/2} 2\pi \sin \theta d\theta \\ &= \frac{1}{3} p = -4\ell^2 E e^{j\omega t}/3L\omega^2. \end{aligned}$$

Therefore, we have

$$\chi_{eav} = -4\ell^2/3L\omega^2. \quad (13)$$

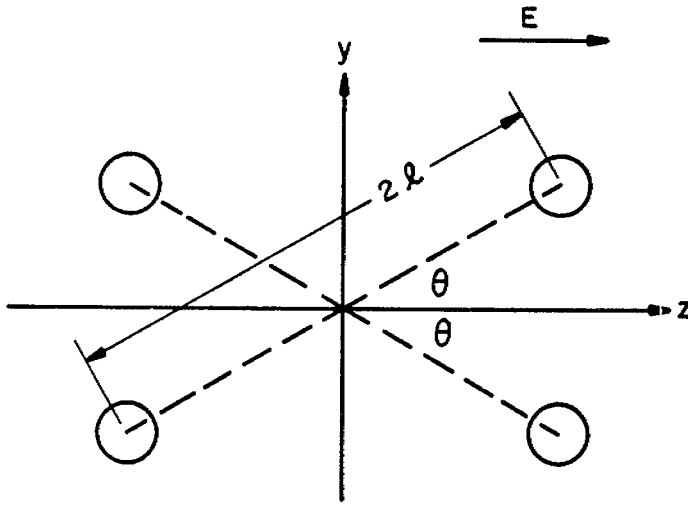


Figure 3. Two dipoles oriented in the θ and $-\theta$ directions.
The y components of the two dipoles cancel.

Now assuming that $\chi_{\text{may}} = 0$, the index of refraction of the artificial dielectric would be

$$n = \left[1 - \frac{4N\ell^2}{3\epsilon_0 L\omega^2} \right]^{1/2}$$

and the intrinsic impedance would be

$$\eta = \left[\mu_0 / \epsilon_0 (1 - \frac{4N\ell^2}{3\epsilon_0 L\omega^2}) \right]^{1/2}$$

In the case of tenuous plasma (ionized high-altitude air) we have an index of refraction given by

$$n = (1 - Ne^2 / \epsilon_0 m \omega^2)^{1/2} = (1 - 3.18 \cdot 10^9 N / \omega^2)^{1/2} \quad (14)$$

where N is the electron density in cm^{-3} , m is the electron mass, and e is the electron charge. Therefore, if we want to simulate a tenuous plasma corresponding to electron density N , we can determine the length 2ℓ and the inductance L of our inductively loaded dipoles with the relation

$$\frac{N\ell^2}{\epsilon_0 L} = \frac{3}{4} \frac{Ne^2}{\epsilon_0 m} = 2.39 \cdot 10^9 N \text{ sec}^{-2}$$

or

$$\frac{N\ell^2}{L} = 2.11 \cdot 10^{-2} N \text{ sec}^{-2} \text{ F/m} \quad (15)$$

where N is the density of artificial dielectric dipoles in meter⁻³, ℓ is in meters, and L is in henrys.

Next, we note that by introducing a resistance into our dipole we can simulate the imaginary part of the index of refraction that arises because of the collisions, ν , per second between the plasma electrons and the atmospheric molecules. Figure 1 shows that the voltage between the dipole spheres is

$$2\ell E e^{j\omega t} = L \frac{d^2 q}{dt^2} + R \frac{dq}{dt}$$

where as before we assume $L\omega \gg 1/C\omega$. Again, we can assume that the charge on the capacitance between the two spheres varies as

$$q = Q e^{j\omega t}.$$

Then

$$2\ell E e^{j\omega t} = LQ(-\omega^2)e^{j\omega t} + RQj\omega e^{j\omega t}$$

and

$$Q = -2\ell E / (L\omega^2 - jR\omega)$$

or

$$q = -2\ell E e^{j\omega t} / (L\omega^2 - jR\omega).$$

The dipole moment along the axis of the inductive dipole in figure 1 is then

$$p = 2\ell q = -4\ell^2 E e^{j\omega t} / (L\omega^2 - jR\omega).$$

We see by analogy with the purely inductive dipole

$$p_{av} = \frac{1}{3} p = -4\ell^2 E e^{j\omega t} / 3(L\omega^2 - jR\omega).$$

Therefore, we have

$$\chi_{\text{eav}} = -4\ell^2/3(L\omega^2 - jR\omega) \quad (16)$$

and

$$\epsilon_p = \epsilon_0 \left[1 - 4\ell^2 N / 3\epsilon_0 L \omega^2 (1 - jR/\omega L) \right] \quad (17)$$

$$= \epsilon_0 \left(1 - \frac{\frac{4}{3} \frac{\ell^2 N}{\epsilon_0 L}}{\left(\frac{R}{L}\right)^2 + \omega^2} + j \frac{\frac{4}{3} \frac{\ell^2 N}{\epsilon_0 L} \left(\frac{R}{L}\right) \frac{1}{\omega}}{\left(\frac{R}{L}\right)^2 + \omega^2} \right). \quad (18)$$

Finally, we note that if equations (3) and (4) are satisfied, we have a one to one correspondence between equations (1) and (18).

2.2 Explicit Consideration of Dipole Capacitance

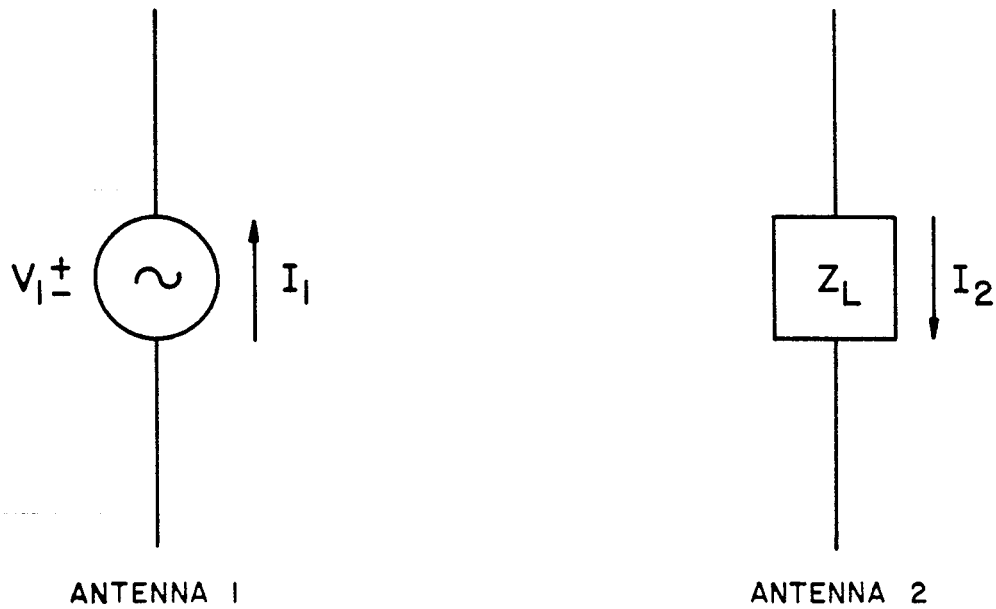
Up to this point we have assumed that the inductance used to load the short dipole dominated the behavior of the dipole. We will now examine this assumption in more detail. The arguments presented here are basically due to Harrington.¹⁵ Consider two short dipole antennas as shown in figure 4. Antenna 1 is excited by a current source I_1 ; antenna 2 is loaded at its center with an impedance Z_L . The currents and voltages of the two dipoles can be related by the standard impedances of a two-port network:

$$\begin{aligned} V_1 &= Z_{11} I_1 - Z_{12} I_2 \\ V_2 &= Z_{21} I_1 - Z_{22} I_2. \end{aligned} \quad (19)$$

The voltage V can be expressed in terms of Z_L and I_2 : $V_2 = Z_L I_2$. Then we can express the current passing through the load Z_L in terms of the current source driving antenna 1; the transfer impedance Z_{21} ; the driving point impedance of antenna Z , Z_{22} ; and the load impedance, Z_L :

$$I_2 = \frac{Z_{21} I_1}{(Z_L + Z_{22})}. \quad (20)$$

We next make use of the reaction concept, first introduced by Rumsey.^{16,17} Rumsey defined reaction of field a on the source b , $\{a,b\}$, with the following integral:



$$V_1 = Z_{11} I_1 - Z_{12} I_2$$

$$V_2 = Z_{21} I_1 - Z_{22} I_2$$

Figure 4. Two short dipole antennas.

$$\{a,b\} = \iiint (\underline{E}^a \cdot \underline{J}^b - \underline{H}^a \cdot \underline{M}^b) dv$$

where \underline{J}^b is the electric current density of source b and \underline{M}^b is the magnetic current density of source b. In this notation the reciprocity theorem is:

$$\{a,b\} = \{b,a\}.$$

For a current source I_b , we can obtain

$$\{a,b\} = \int \underline{E}^a \cdot \underline{I}^b d\ell = I^b \int \underline{E}^a \cdot d\underline{\ell} = -V^a I^b. \quad (21)$$

The transfer impedance in equation (19) is defined by

$$Z_{ij} = V_{ij}/I_j$$

where V_{ij} is the voltage at terminal i produced by the current source at terminal j. In equation (21) we indicate that

$$\{j,i\} = -V_{ij} I_i,$$

therefore, we obtain by eliminating V_{ij} and using the reciprocity theorem

$$Z_{ij} = -\frac{1}{I_i I_j} \iint E_i J_j ds. \quad (22)$$

We next remove dipole number 1 to minus infinity so that the electric field, E_1 , at dipole number 2 is a plane wave. King¹⁸ shows that for a short dipole of length B , i.e. for $(\pi/\lambda) B < 1/2$, we can assume an induced current distribution on dipole 2 of the form:

$$I_2^1(z) = I_2 \left(1 - \frac{2}{B} |z|\right). \quad (23)$$

Equation (22) then yields:

$$Z_{12} = \frac{E_1 B}{2I_1} = Z_{21} \quad (24)$$

and from equation (20) we obtain:

$$I_2 = \frac{Z_{21} I_1}{(Z_L + Z_{22})} = \frac{E_1 B}{2(Z_L + Z_{22})}.$$

Equation (23) then can be expressed as

$$I_2^1(z) = \frac{E_1 B}{2(Z_L + Z_{22})} \left(1 - \frac{2}{B} |z|\right). \quad (25)$$

The conservation of charge along dipole number 2 can be expressed as

$$\frac{d I_2^1(z)}{dz} + j \omega q(z) = 0, \quad (26)$$

where $q(z)$ is now the charge per unit length, and therefore the charge distribution along dipole 2 is:

$$q(z) = \frac{j}{\omega} \frac{d I_2^1(z)}{dz}. \quad (27)$$

The dipole moment along antenna 2, p , is given by the following integral:

$$p = \int_{-\frac{B}{2}}^{\frac{B}{2}} q(z) z dz. \quad (28)$$

Expressions (25), (26), and (28) then yield:

$$P = \frac{-j E_1 B^2}{4\omega(j\omega L + Z_{22})}. \quad (29)$$

If we allow χ to be the polarizability of the dipole we have:

$$p = E \cdot \chi \quad (30)$$

or

$$\chi = \frac{-j B^2}{4\omega(j\omega L + Z_{22})}. \quad (31)$$

Equation (31) is essentially the same as the result we obtained with the simple quasi-static model, except for the presence of the driving point impedance Z_{22} in the denominator. (The factor 4 in the denominator occurs because we have not capacitively end-loaded the dipole as in figure 1.)

King^{19,20} derives a value for the impedance Z_{22} of a short dipole:

$$Z_{22} = \frac{\eta}{2\pi} \left[\frac{\left(\frac{\omega}{c}\right)^2 B^2}{12} - j \frac{4 \ln \left(\frac{B}{A}\right) - 6.78}{\left(\frac{\omega}{c}\right)b} \right]. \quad (32)$$

Here η is the impedance of free space, $120 \pi \Omega$, B is the length of the dipole, and A is the dipole radius.

Up to this point we have considered the incident electric field E , to be parallel to the short inductively-loaded dipole. Of course, the current and charge distribution along the dipole is a function of the orientation of the receiving antenna with respect to the surface of constant phase of the incident electric field. King¹⁹ indicates that for a short receiving antenna (with a triangular current distribution) the projection of the electric field onto the antenna, multiplied by the actual half length of the antenna, gives the emf of the equivalent circuit. That is equation (24) is modified to

$$Z_{12} = Z_{21} = \frac{E_1 B}{I_{12}} \cos \theta \quad (33)$$

where θ is the angle between the incident electric field vector and the antenna. For example, $\theta = 0^\circ$ when the antenna lies in the surface of constant phase. We can now use the same orientation arguments that we used in the development of our quasi-static model which

ignored the self impedance Z_{22} . If we wish to calculate the polarization in the direction of the incident electric field when the E_1 vector is not parallel to the dipole, we must introduce another $\cos \theta$ and integrate over all directions. Therefore, as before

$$P_{av} = \frac{1}{3} P$$

and

$$P_{av} = \chi_{av} E$$

or

$$\chi_{av} = \frac{-j B^2}{12\omega(j\omega L + Z_{22})} \quad (34)$$

If we set $Z_{22} = 0$, $B = 2\ell$, and end-load the dipole so that the current distribution is uniform and not triangular, we obtain the same result as given by equation (13).¹⁸

The appearance of Z_{22} in the denominator of expression (34) is inconsistent with our desire to model a simple Lorentzian plasma. Specifically, when the frequency is such that

$$\omega L = \left[\frac{4 \ln\left(\frac{B}{A}\right) - 6.78}{\left(\frac{\omega}{c}\right) B} \right] \left(\frac{n}{2\pi}\right) \quad (35)$$

the artificial dielectric will pass through a resonance. We can only use the inductively-loaded dipoles to simulate a plasma if $\omega L \gg Z_{22}$. We will discuss the effect of Z_{22} in a subsequent section. An insight into the limitations imposed by the dipole self-impedance can be obtained by calculating χ_{av} for some realistic frequencies and dipole parameters.

2.3 Mutually Perpendicular Dipole Scatterers

Our arguments presented so far assumed that the distance between the inductively-loaded dipoles is great enough so that their interaction can be neglected. The use of equation (8) is based on the assumption of negligible interaction between scattering objects. A way of increasing the value of N in (8) by a factor of 3 and still not violate the assumption of negligible interaction of neighboring scatterers is to construct each scatterer out of three mutually-perpendicular inductively-loaded dipoles. By using essentially quasi-static arguments it is easy to see that three mutually-perpendicular dipoles with a common center point do not interact.

Consider just two perpendicular dipoles as shown in figure 5. By symmetry the current distribution along the two arms of dipole 1 is symmetrical and equal in magnitude. Therefore, the charge distribution along the opposite arms is equal in magnitude but of opposite sign. Using a static argument the electric field produced by the charge distribution along dipole 1 is seen to be perpendicular to the direction of dipole 2. The dipoles therefore do not interact. Similar reasoning applies to a dipole that is mutually perpendicular to dipoles 1 and 2 and centered at the intersection of dipoles 1 and 2. These quasi-static arguments are consistent with the more rigorous arguments presented for skew-angled dipoles by Richmond.²¹ If we substitute three mutually-perpendicular dipoles for the single randomly-distributed dipoles we simply multiply the average value of the polarizability given in equation (34) by 3 and obtain

$$\chi_{av3} = \frac{-j B^2}{4\omega(j\omega L + Z_{22})}. \quad (36)$$

By constructing our scatterers out of three mutually-perpendicular inductively-loaded dipoles we accomplish more than simply increasing the number of scatterers by three: the polarizability of the scattering centers is made to be independent of scatterer orientation. To be specific, the scatterer, consisting of three identical, short, mutually-perpendicular dipoles centered at the origin with a dipole along each axis, can be described with the following simple dyadic:

$$\underline{\underline{\chi}} = \chi (\hat{i} \hat{i} + \hat{j} \hat{j} + \hat{k} \hat{k}) = \chi \underline{\underline{I}}.$$

The dipole moment induced by an arbitrary field \vec{E} is then

$$\begin{aligned} \vec{p} &= \underline{\underline{\chi}} \cdot \vec{E} \\ &= \underline{\underline{\chi}} \cdot E (\hat{i} \sin \theta \cos \phi + \hat{j} \sin \theta \sin \phi + \hat{k} \cos \theta) \\ &= \chi E (\hat{i} \sin \theta \cos \phi + \hat{j} \sin \theta \sin \phi + \hat{k} \cos \theta) \end{aligned} \quad (37)$$

but $(\sin \theta \cos \phi)^2 + (\sin \theta \sin \phi)^2 + \cos^2 \theta = 1$. Therefore, the magnitude of the dipole moment is $\propto E$ and its direction is in the direction of the electric field regardless of the orientation of the scatterer.

In order to gain insight into the foregoing result we can consider a relatively simple situation in more detail. Figure 6 illustrates two perpendicular inductively-loaded dipoles in the plane of the page. Let the \vec{E} vector of the incident plane wave also be in the plane of the page. The third dipole is perpendicular to the plane of the page, and therefore is perpendicular to the \vec{E} vector and does not interact with the E field. As shown in the figure, the Poynting vector \vec{S} of the incident plane wave is also in the plane of the page. The voltage developed across the load of dipole number 1 is then proportional to $E \cos \theta$ and the separation of

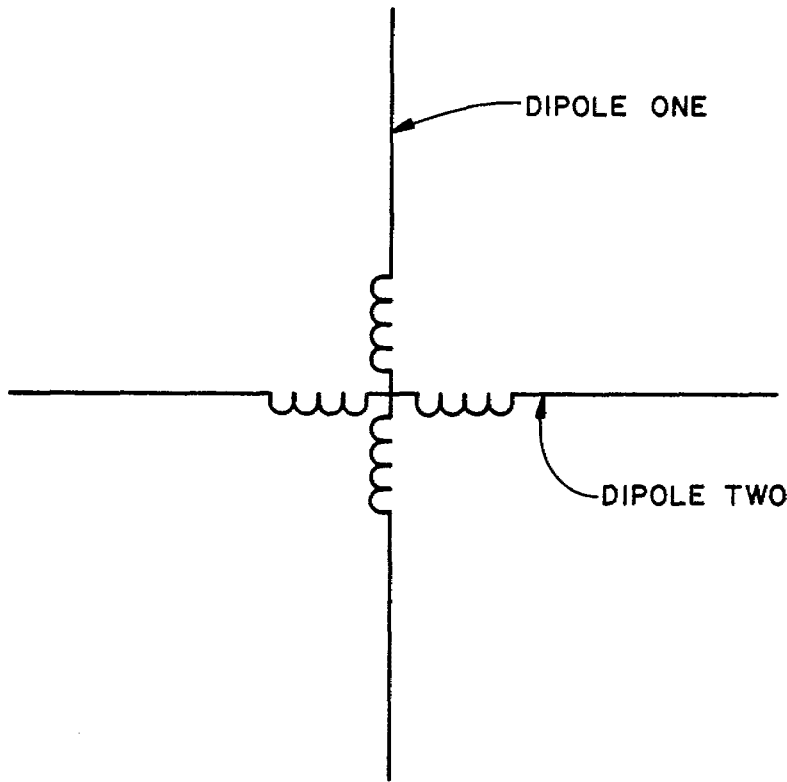


Figure 5. Two perpendicular inductively-loaded dipoles do not interact.

charge on dipole number 1 in the direction of the incident E vector is proportional to $\cos^2\theta$, that is $p_{1,E||} = K \cos^2\theta$. A corresponding argument (see fig. 7) leads to the conclusion that the dipole moment of dipole number 2 in the direction of the incident field E is given by $p_{2,E||} = K \sin^2\theta$. The total dipole moment in the direction of the vector E of dipoles 1 and 2 is, therefore, given by

$$\begin{aligned}
 P_{E||} &= P_{1,E||} + P_{2,E||} = K \cos^2\theta + K \sin^2\theta \\
 &= K = \frac{-j B^2 E}{4\omega(j\omega L + Z_{22})}.
 \end{aligned}
 \tag{38}$$

Let us now consider the polarization perpendicular to the \vec{E} vector. As shown in figure 8 the voltage developed across the load on dipole 1 is proportional to $E \cos \theta$ and the dipole moment perpendicular to the E field or parallel to the S vector is $p_{1,E\perp} = -K \cos \theta \sin \theta$. As shown in figure 7, since the voltage across the load on dipole 2 is proportional to $E \sin \theta$, the dipole moment component of dipole two perpendicular to the incident field is

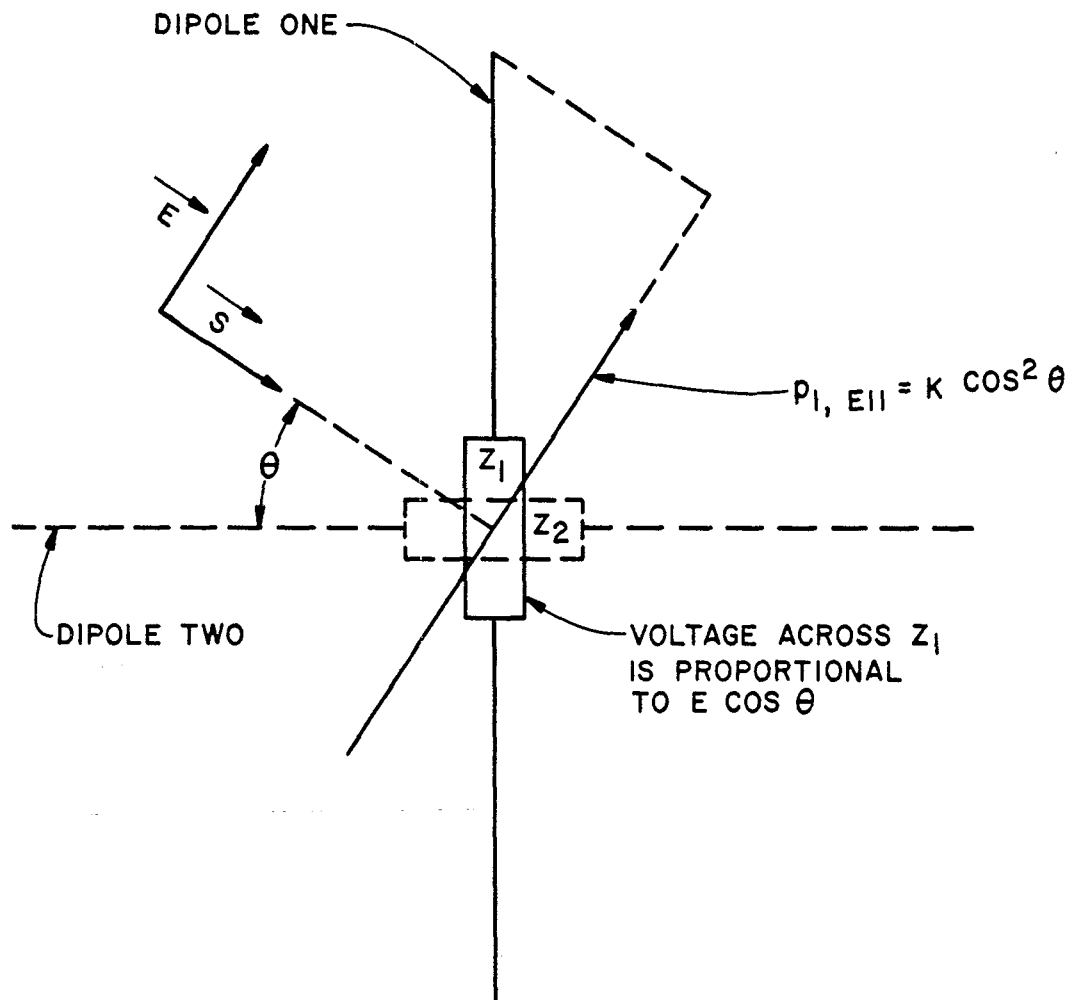


Figure 6. The vector $p_{1,E11}$ is the dipole moment component of dipole 1 that is parallel to the incident electric field.

$$p_{2,E1} = K \sin \theta \cos \theta.$$

So for the total polarization perpendicular to \vec{E} we have

$$\begin{aligned} p_{\perp E} &= p_{1,E1} + p_{2,E1} \\ &= K (-\sin \theta \cos \theta + \sin \theta \cos \theta) \\ &= 0. \end{aligned} \tag{39}$$

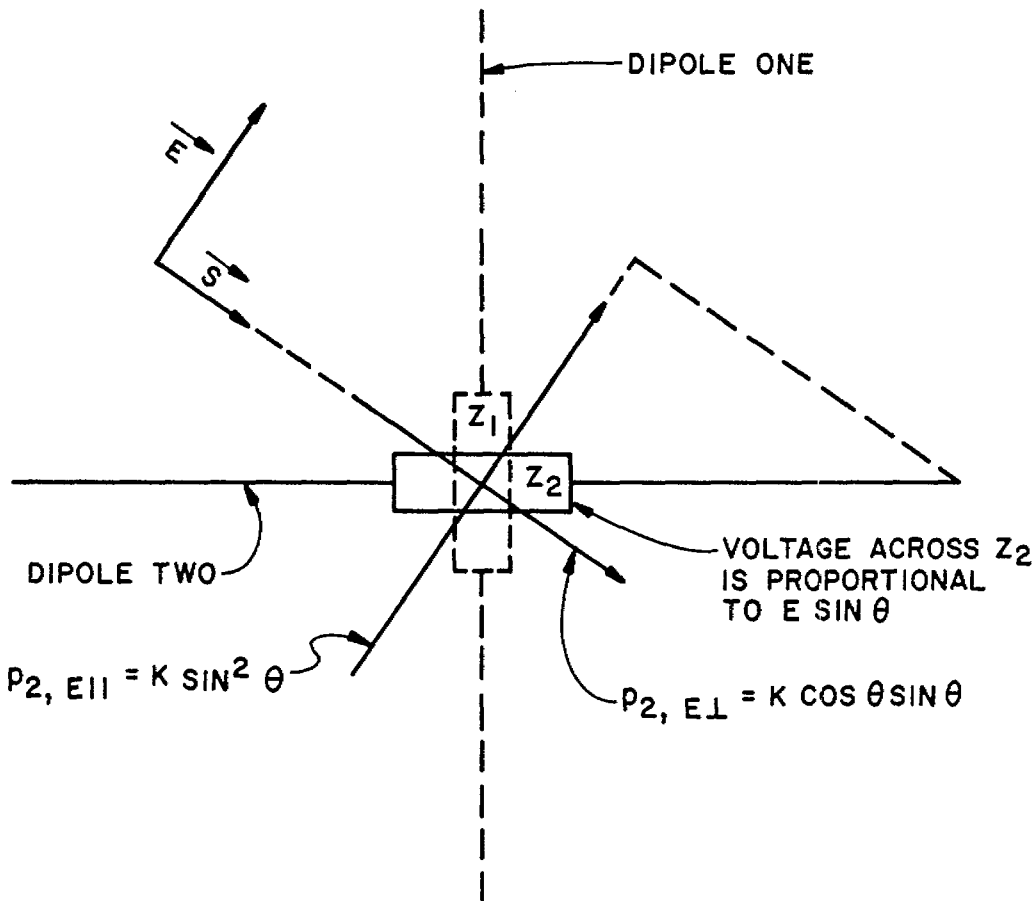


Figure 7. The dipole moment of dipole 2 can be resolved into components parallel and perpendicular to the incident electric field.

In summary, we see that the rather tedious arguments leading to equations (38) and (39) are consistent with the result of equation (37). Of course, as the length of the dipoles is increased, the simple trigonometric dependence for the current or charge distribution does not hold, and the polarization is not independent of the direction of the incident electric field.

2.4 Coupling of Scatterers

The dipole interaction of the scattering objects, each consisting of three mutually-perpendicular and centered, inductively-loaded dipoles, will be considered next. The starting point for the discussion of the coupling of scattering objects in both real and artificial dielectrics is the formula of Lorentz for the field within a hollow spherical cavity (centered at a particular molecule or scatterer) cut out of the dielectric

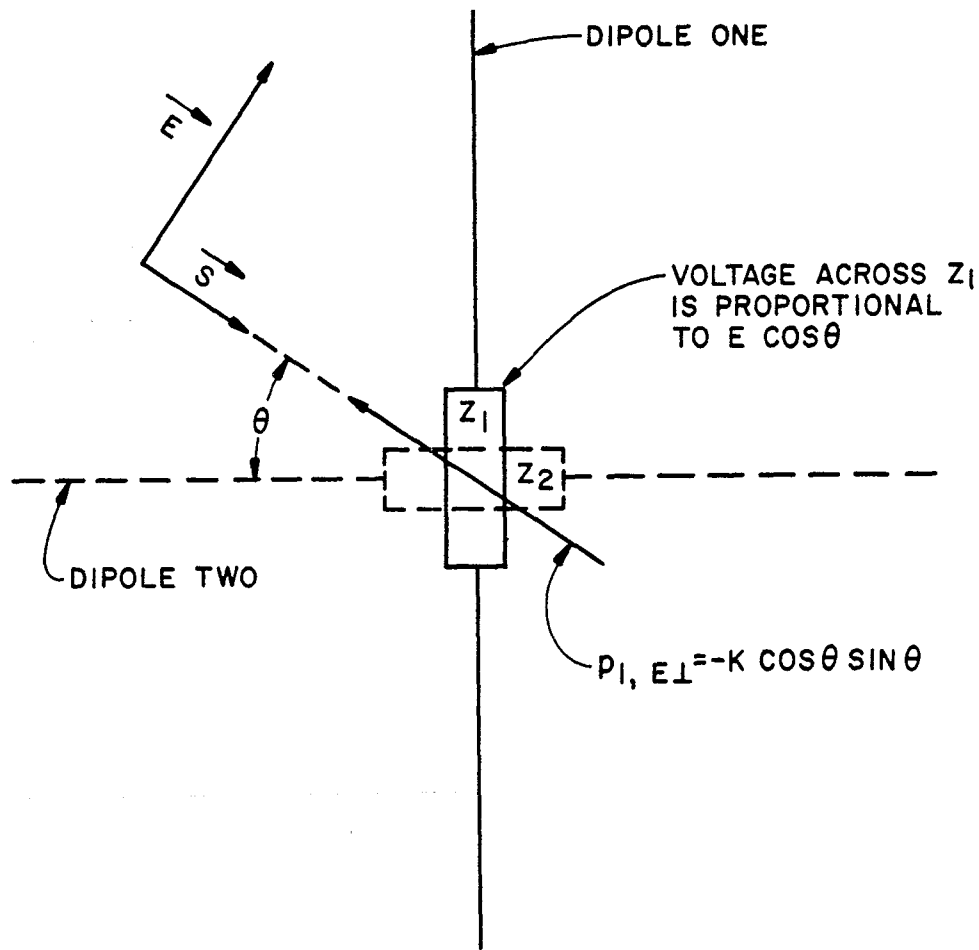
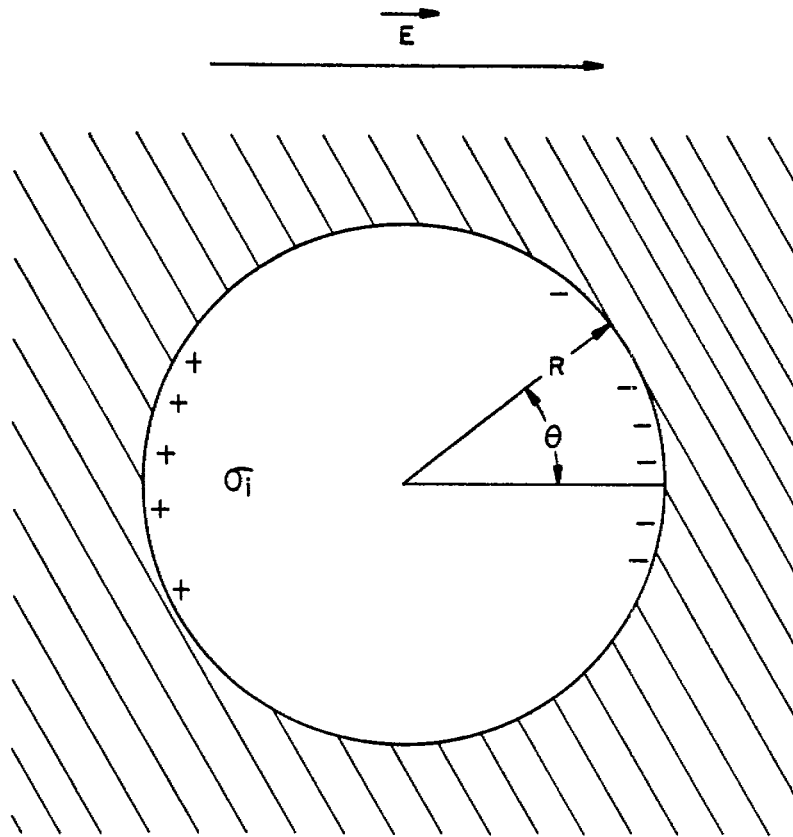


Figure 8. The vector $p_{1, E_{\perp}}$ is the dipole moment component of dipole 1 that is perpendicular to the incident field.

(fig. 9). The displacement vector D normal to the dielectric surface between the sphere and the cavity must be continuous; therefore, the magnitude of P normal to the cavity surface equals the negative of the induced surface charge density σ_1 . We may write $\sigma_1 = -|\vec{P}| \cos \theta$. The field inside the cavity due to σ_1 can be calculated at the center of the cavity with Coulomb's law:

$$E_s = \int_s \frac{\sigma_1 ds \cos \theta}{4\pi \epsilon_0 R^2}$$



$$\begin{aligned}
 E_S &= \int \frac{\sigma_i \, dS}{4\pi\epsilon_0 R^2} \cos\theta \\
 &= \int_0^\pi \frac{|\vec{P}| \cos\theta}{4\pi\epsilon_0 R^2} \cos\theta \, 2\pi R^2 \sin\theta \, d\theta \\
 &= \frac{|\vec{P}|}{3\epsilon_0}
 \end{aligned}$$

Figure 9. Spherical cavity in dielectric.

$$\begin{aligned}
&= \int_0^\pi \frac{|\vec{P}| \cos \theta \cos \theta 2\pi R^2 \sin \theta d\theta}{4\pi \epsilon_0 R^2} \\
&= \frac{|\vec{P}|}{2\epsilon_0} \int_0^\pi \cos^2 \theta \sin \theta d\theta \\
&= \frac{|\vec{P}|}{3\epsilon_0}.
\end{aligned}$$

Therefore, the local field at the center of the cavity at a particular molecule or scatterer is

$$\vec{E}_{loc} = \vec{E} + \frac{1}{3\epsilon_0} \vec{P} + \vec{E}_2.$$

Here E is the ordinary macroscopic field, P is the polarization of the dielectric, and E_2 is the mean field due to the matter within the sphere itself (exclusive of the central scatterer). The magnitude of E_2 will depend on the distribution of scatterers within the spherical cavity. Lorentz showed that if the molecules are arranged in a cubical array, E_2 will be zero. Lorentz also indicated that to a certain degree of approximation $E_2 = 0$ for such isotropic bodies as glass, fluids, and gases. We will discuss this approximation in a later section.

Assuming that $E_2 = 0$, we obtain the following value for the local field at a scatterer:

$$\vec{E}_{loc} = \vec{E} + \vec{P}/3\epsilon_0 \tag{40}$$

The dipole moment of a scatterer is then $\vec{p} = \chi_{av} \vec{E}_{loc}$, but,

$$\vec{P} = \vec{p} N = \chi_{av} N \vec{E}_{loc}$$

where N is the number density of scatters per unit volume. According to the usual notation:

$$\epsilon \vec{E} = \epsilon_0 \vec{E} + \vec{P}.$$

Therefore

$$\vec{P} = \vec{E} (\epsilon - \epsilon_0)$$

and

$$\begin{aligned}\vec{P} &= \chi_{av3} N \vec{E}_{loc} = \chi_{av3} N (\vec{E} + \vec{P}/3\epsilon_0) \\ &= \chi_{av3} N \left(\vec{E} + \frac{\vec{E}(\epsilon_1 - \epsilon_0)}{3\epsilon_0} \right).\end{aligned}\quad (41)$$

This is the Clausius-Mossotti relation. Equation (41) can be manipulated to yield:

$$\epsilon = \epsilon_0 \frac{1 + 2 N \chi_{av3}/3\epsilon_0}{1 - N \chi_{av3}/3\epsilon_0}.\quad (42)$$

The above expression is only valid when the local electric field E_{loc} at a scattering obstacle can be expressed as

$$\vec{E}_{loc} = \vec{E} + \vec{P}/(3\epsilon_0)\quad (43)$$

where E is the space average field inside the artificial dielectric.

The local fields for simple tetragonal and hexagonal lattices have also been calculated by a number of workers. Collin^{7,22} considers a three-dimensional array of y-directed unit dipoles at $x = na$, $y = mb$, and $z = sc$. He excludes the dipole at $x = y = z = 0$ and calculates the local field at $x = y = z = 0$. The potential due to a unit dipole at x_0, y_0, z_0 is

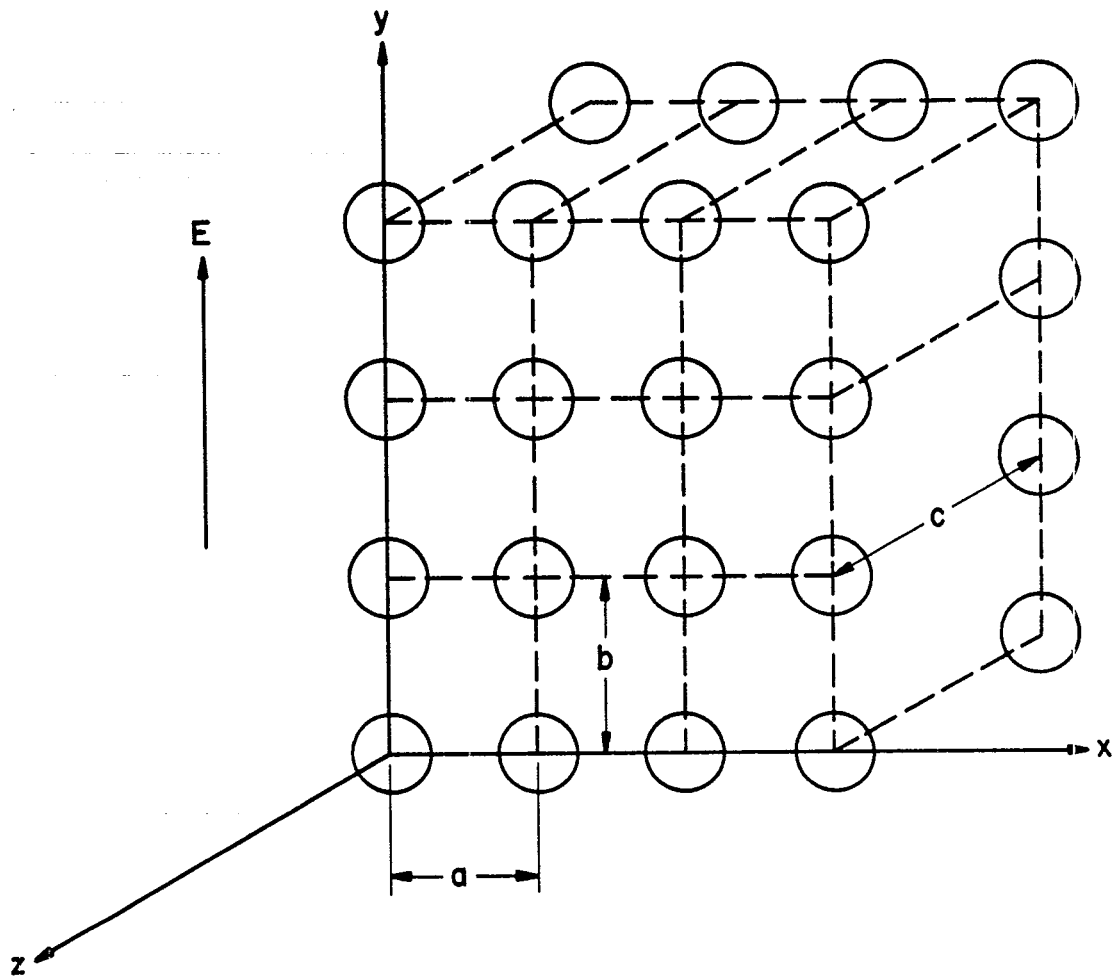
$$\phi = \frac{\hat{j} \cdot \vec{r}}{4\pi \epsilon_0 r^3}\quad (44)$$

where $r = [(x - x_0)^2 + (y - y_0)^2 + (z - z_0)^2]^{1/2}$. For the array of y-directed dipoles we then have (fig. 10)

$$\phi = \frac{1}{4\pi\epsilon_0} \sum_{n=-\infty}^{\infty} \sum_{s=-\infty}^{\infty} \sum'_{m=-\infty}^{\infty} \frac{y - mb}{[(x-na)^2 + (y-mb)^2 + (z-sc)^2]^{3/2}}\quad (45)$$

where the prime indicates the omission of the $n = m = s = 0$ term. The effective polarizing field at $x = 0, y = 0, z = 0$ will then be $E + E_i$, where E is the external applied field and where

$$E_i = - \left. \frac{\partial \phi}{\partial y} \right|_{x = y = z = 0}$$



CUBIC LATTICE $a = b = c$

TETRAGONAL LATTICE $a = c \neq b$

HEXAGONAL LATTICE $a \neq b \neq c$

Figure 10. Three-dimensional array of inductively-loaded dipoles enclosed in styrofoam spheres.

$$= \frac{1}{4\pi\epsilon_0} \sum_{m=-\infty}^{\infty} \sum_{n=-\infty}^{\infty} \sum_{s=-\infty}^{\infty} \frac{2(mb)^2 - (na)^2 - (sc)^2}{[(mb)^2 + (na)^2 + (sc)^2]^{5/2}} \quad (46)$$

Note that the above expression is not only evaluated inside the Clausius-Mossotti sphere, but over all space. We therefore do not have to consider a contribution from the inside surface of the sphere.

Collin evaluates expression (46) and obtains

$$E_i = \frac{1}{\epsilon_0} \left\{ \frac{1.201}{\pi b^3} - \frac{8\pi}{b^3} \left[K_0 \left(\frac{2\pi c}{b} \right) + K_0 \left(\frac{2\pi a}{b} \right) \right] \right\} \quad (47)$$

where K_0 is the so-called modified Bessel function of order zero. Equation (47) is for unit dipoles. In our case of inductively-loaded dipoles we would have

$$E_i = \frac{1}{\epsilon_0} \left\{ \frac{1.201}{\pi b^3} - \frac{8\pi}{b^3} \left[K_0 \left(\frac{2\pi c}{b} \right) + K_0 \left(\frac{2\pi a}{b} \right) \right] \right\} \chi_{av3} \quad (48)$$

or

$$E_{loc} = E + \frac{1}{\epsilon_0} \left\{ \frac{1.201}{\pi b^3} - \frac{8\pi}{b^3} \left[K_0 \left(\frac{2\pi c}{b} \right) + K_0 \left(\frac{2\pi a}{b} \right) \right] \right\} \left(\frac{j B^2}{4\omega(j\omega L + Z_{22})} \right) \quad (49)$$

The above equation corresponds to a cubic lattice if $a = b = c$, a tetragonal lattice if only two of the quantities are equal, and a hexagonal lattice if none of the quantities, a , b , or c are equal. In the case of the cubic lattice we find that

$$E_{loc} = E + \frac{1.06 N}{\pi \epsilon_0} \chi_{av3} \quad (50)$$

and, therefore

$$\epsilon = \epsilon_0 \frac{1 + \frac{2.08 N}{\pi \epsilon_0} \chi_{av3}}{1 - \frac{1.06 N}{\pi \epsilon_0} \chi_{av3}} \quad (51)$$

which is to be compared with equation (42).

2.5 Deviations from the Clausius-Mossotti Equation Due to Randomness of Scatterers

J.K. Kirkwood^{23,24} has calculated the deviations that one might expect from equation (40) in the case of a random distribution of molecules consisting of hard spheres. Specifically, Kirkwood considered a molecular interaction potential of the form

$$\begin{aligned} W(r) &= \infty & 0 \leq r \leq a \\ &= 0 & r > a \end{aligned} \tag{52}$$

where a is the diameter of a molecule.

Kirkwood's model is not wholly applicable to an artificial dielectric formed by dumping spherical scatterers into a container because the scatterers do not necessarily assume a completely random distribution. For example, depending, among other factors, on how smooth they are, the spheres can arrange themselves into various specific lattices or combinations of lattices. The different lattices can even correspond to different dipole number densities.

It is interesting to note that statistical mechanical averaging based on the molecular interaction equation (52) yields a value of the permittivity that is not a function of the thermodynamic temperature T . This follows because the value of the exponential term $\exp[-W(r)/kT]$ is either 0 or 1. In a gas or fluid the averaging can be over time; in our static collection of scattering dipoles the averaging would have to be over an ensemble of different containers each filled with a aggregation of spherical dipole scatterers. Kirkwood's approach can be summarized as follows: As in the lattice case, the local field is obtained by summing over the potentials due to individual dipoles. We can say that the effective polarizing field E_{loci} at scatterer i will be given by $E + E_i$, where E is the external applied field and E_i is given by the sum over N individual dipoles:

$$\vec{E}_i = - \sum_{\substack{k=1 \\ \neq i}}^N \underline{T}_{ik} \cdot \vec{p}_k \tag{53}$$

where the dipole-interaction dyadic is given by

$$\underline{T}_{ik} = \frac{1}{4\pi\epsilon_0} \frac{1}{r_{ik}^3} \left[\underline{I} - 3 \frac{\vec{r}_{ik} \vec{r}_{ik}}{r_{ik}^2} \right] \tag{54}$$

The polarization of an individual scatterer is given by

$$\begin{aligned}\vec{p}_i &= \epsilon_0 \alpha \underline{\underline{E}}_{1\text{loc}i} = \epsilon_0 \alpha \cdot (\vec{E} + \vec{E}_i) \\ &= \epsilon_0 \alpha \vec{E} - \epsilon_0 \alpha \sum \underline{\underline{T}}_{ik} \cdot \vec{p}_k\end{aligned}\quad (55)$$

We therefore have N simultaneous equations

$$\vec{p}_i + \alpha \epsilon_0 \sum \underline{\underline{T}}_{ik} \cdot \vec{p}_k = \alpha \epsilon_0 \vec{E} \quad i = 1, \dots, N$$

that would have to be solved in order to obtain $E_{1\text{loc}i}$ for each of the individual scatterers in the distribution of N scatterers in volume V . We can average the N equations and obtain

$$\overline{\vec{p}} + \alpha \epsilon_0 \sum \overline{\underline{\underline{T}}_{ik} \cdot \vec{p}_k} = \alpha \epsilon_0 \vec{E} \quad (56)$$

Kirkwood^{23,24} introduced the following fluctuation term

$$\vec{n} = \sum_{\substack{i=1 \\ i \neq k}}^N (\underline{\underline{T}}_{ik} \cdot \vec{p}_k - \overline{\underline{\underline{T}}_{ik} \cdot \vec{p}_k}) \quad (57)$$

and obtained

$$\overline{\vec{p}} + \alpha \epsilon_0 \sum \overline{\underline{\underline{T}}_{ik} \cdot \vec{p}} + \vec{n} \alpha \epsilon_0 = \alpha \epsilon_0 \vec{E} \quad (58)$$

If we can assume that

$$\overline{\underline{\underline{T}}_{12} \cdot \vec{p}_1} = \overline{\underline{\underline{T}}_{12}} \cdot \overline{\vec{p}_1} \quad (59)$$

the fluctuation \vec{n} is equal to zero and

$$\overline{\vec{p}} + \alpha \epsilon_0 \overline{\vec{p}} \cdot \sum \overline{\underline{\underline{T}}_{ik}} = \alpha \epsilon_0 \vec{E}. \quad (60)$$

Converting to the equivalent scalar equation we obtain:

$$\overline{p} = \frac{\alpha \epsilon_0 E}{1 + \alpha \epsilon_0 (\sum \overline{\underline{\underline{T}}_{ik}})}, \quad (61)$$

and

$$D = \epsilon E = \epsilon_0 E + P \quad (62)$$

$$= \epsilon_0 E + \frac{N}{v} \bar{p}$$

$$= \epsilon_0 E + \frac{\epsilon_0 \frac{N}{v} \alpha E}{1 + \alpha \epsilon_0 (\sum T_{ik})} \quad (63)$$

The dipole interaction term can be averaged over the volume v to yield:

$$\sum \bar{T}_{ik} = -\frac{1}{3} \frac{N}{v}, \quad (64)$$

also

$$\alpha = \frac{\chi_{av3}}{\epsilon_0} \quad (65)$$

and therefore

$$\epsilon = \epsilon_0 \left\{ 1 + \frac{\frac{N}{v} \alpha}{1 - \frac{1}{3} \frac{N}{v} \alpha} \right\} \quad (66)$$

or

$$\epsilon = \epsilon_0 \frac{1 + \frac{2}{3} \frac{N}{v} \frac{\chi_{av3}}{\epsilon_0}}{1 - \frac{1}{3} \frac{N}{v} \frac{\chi_{av3}}{\epsilon_0}} \quad (67)$$

Equation (67) is to be compared with equations (51) and (42). After considerable mathematical manipulation and a number of approximations, Kirkwood managed to evaluate equation (57) for a substance consisting of a random distribution of hard noninteracting spheres of diameter a :

$$n \approx \left(\frac{1}{9b} - \frac{5}{48v} \right) \frac{N^2 \alpha^2 D}{v} \quad (68)$$

where

$$b = \frac{2\pi N a^3}{3} = 4N \left(\frac{\pi a^3}{6}\right) \\ = 4 \text{ (volume of spherical scatterers).}$$

To obtain a rough estimate of the validity of using the Clausius-Mossotti equation for a random distribution of styrofoam ball dipole scatterers, we can compare the value of n given by equation (68) with the value of n

$$1 - \alpha \sum T_{ik} = 1 + \frac{1}{3} \frac{N\alpha}{v}$$

For the experimental situation discussed in Section 2:

$$\frac{n}{1 - \alpha \sum T_{ik}} = .22$$

and we might expect the Clausius-Mossotti equation to be a reasonable first approximation. Actually, as we have pointed out, Kirkwood's statistical model is not necessarily applicable to our aggregation of dipole scatterers because the dipole scatterers in the artificial dielectric do not necessarily assume a random distribution. The validity of the Clausius-Mossotti equation as applied to our artificial dielectric should really be tested empirically.

3. COMPARISON OF EXPERIMENT WITH THEORY

In order to orient ourselves in regard to the parameters such as the dipole load impedance and Z_{22} we will use equations (36) and (42) to design an artificial dielectric with some actual experiments in mind. The frequency range considered will be dictated by the band pass characteristics of the type 2300 waveguide. The type 2300 waveguide, the largest standard waveguide, has internal dimensions of 23.0 x 11.5 in., a lower cutoff frequency of 2.56×10^8 H, and a recommended upper frequency limit of 4.9×10^8 H. The frequencies in this range are much higher than the values usually quoted for nuclear EMP pulses, but we will consider designing an artificial dielectric to operate at these high frequencies because of the convenience of using waveguide techniques in measuring the properties of an artificial dielectric.

Let us consider the following series of parameters as an orientation exercise. We begin with an artificial dielectric constructed out of scatterers consisting of three mutually-perpendicular inductively-loaded 7-in. long dipoles loaded with a number of different values of inductance. Let the dipole stems have a radius of 0.1 cm. We choose the density of

scatterers to be 264 per cubic meter. This density corresponds to an aggregation of 48 scatterers distributed throughout a rectangular container with dimensions 23 x 11.5 x 41.5 in. Equations (36) and (42) can be employed to calculate the dielectric constant of the artificial dielectric as a function of frequency in the band-pass region of the type 2300 waveguide. Figure 11 shows values of the real part of the permittivity calculated with equations (36) and (42) for a frequency range between 300 and 500 MHz. The four curves correspond to dipole load inductances of 0.4, 0.6, 0.9, and 1.4 μH . The magnitude of the radiation resistance of the dipoles is very small compared to the values of the magnitude of the inductive loads; therefore, the imaginary components of the permittivity are very small.

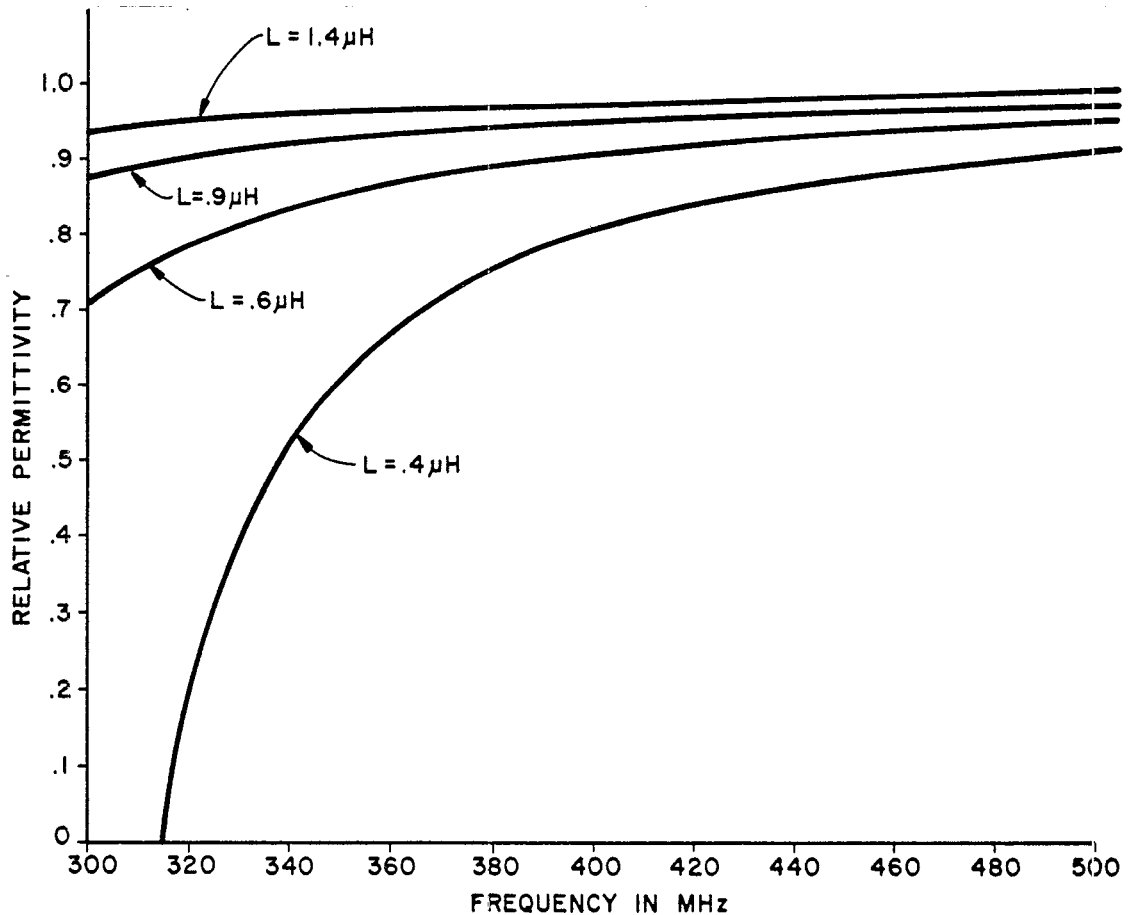


Figure 11. Values of relative permittivity calculated with equations (36) and (42) for a number of different inductive loads. The other parameters are discussed in the text.

If we want to model a Lorentz plasma in which the electrons have a collision frequency $\nu \neq 0$, the load impedance of our dipoles must have a resistive component. Equation (36) then becomes:

$$\chi_{av3} = \frac{-j B^2}{4\omega(j\omega L + R + Z_{22})} \quad (69)$$

where R is the value of the resistance. In figures 12a to 12d we present values of the real part of the permittivity calculated with equations (69) and (42) with $L = 0.4 \mu\text{H}$. The series of four figures shows the effect of different values of the resistive component R on the magnitude of the resonance occurring when $j\omega L = Z_{22}$. Figure 12a, corresponding to a purely inductive load, emphasizes the resonance behavior of the artificial dielectric produced when the load inductance L is in resonance with the capacitive impedance of the dipole. As can be expected the Q of the resonance is reduced by including a resistance in the dipole load impedance.

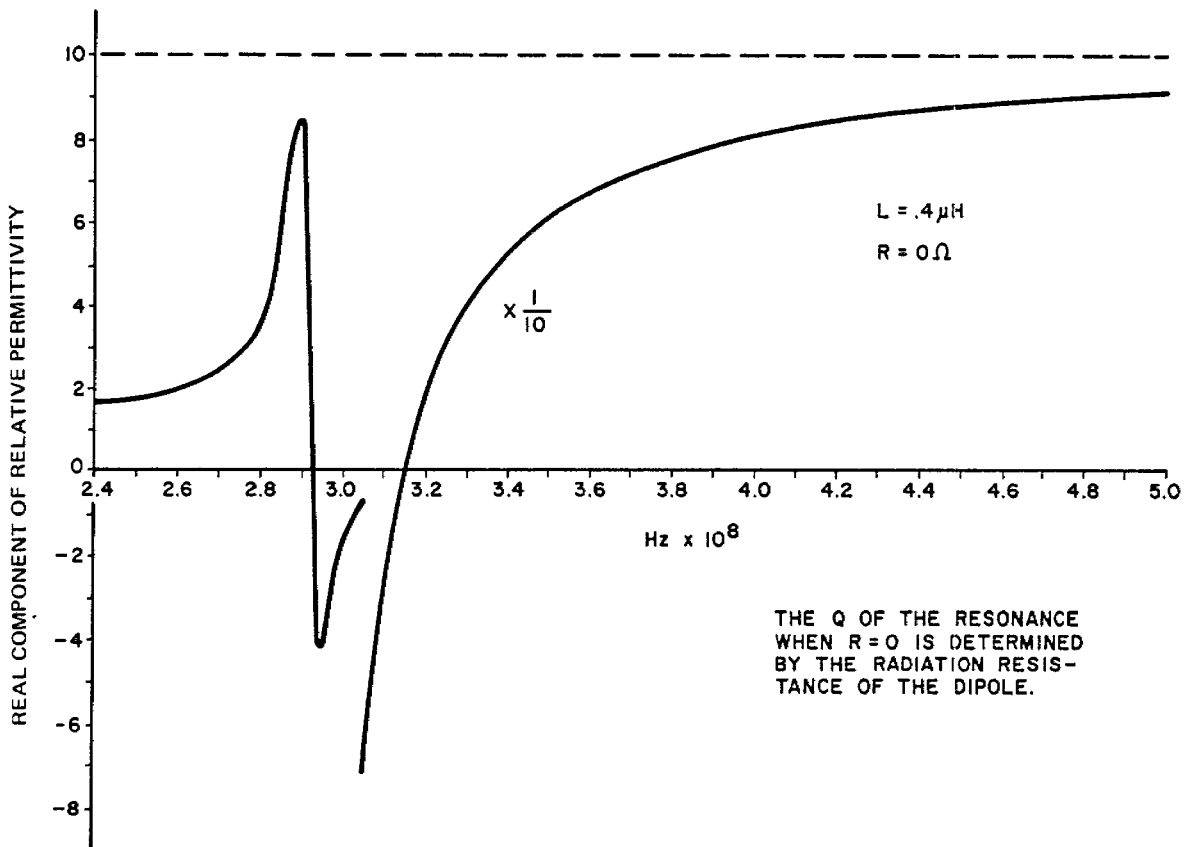


Figure 12a. The real component of relative permittivity calculated with equations (69) and (42). The value used for L is $.4 \mu\text{H}$ and the value used for R is 0Ω . The other parameters are the same as those employed to obtain figure 11.

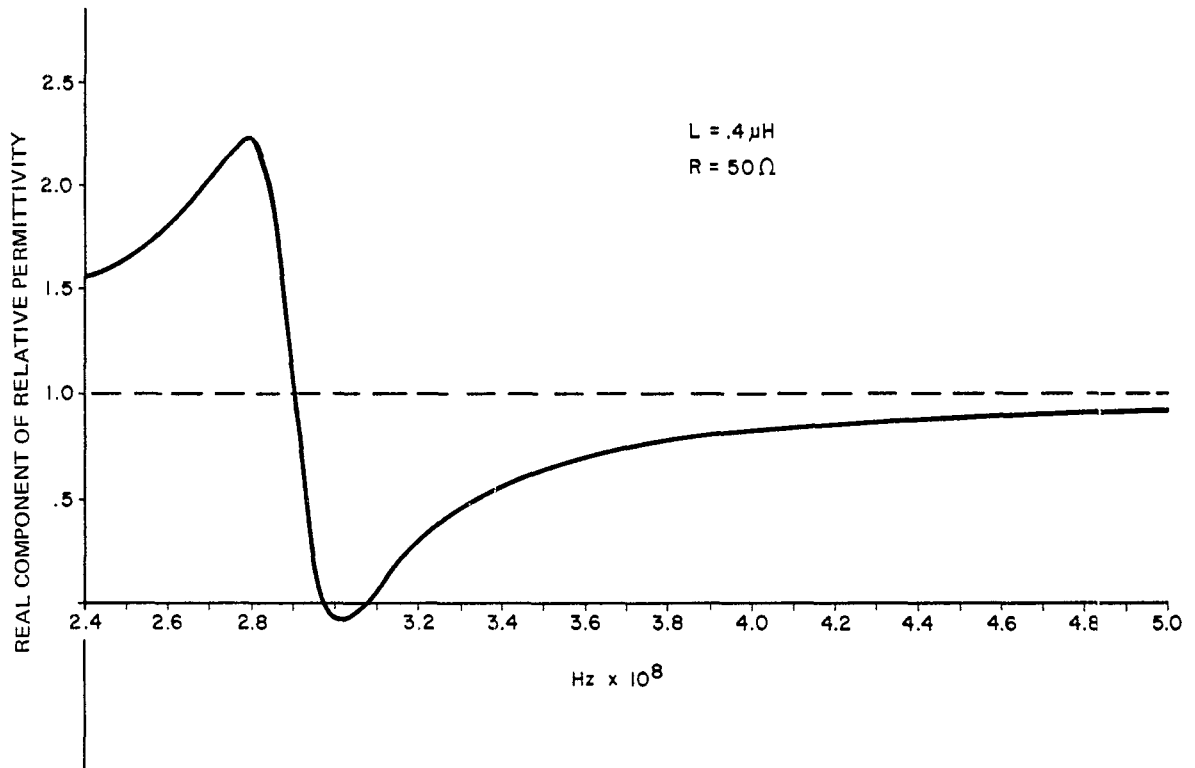


Figure 12b. The real component of relative permittivity calculates with equations (69) and (42). The value used for L is .4 μH and the value used for R is 50 Ω . The other parameters are the same as those employed to obtain figure 11.

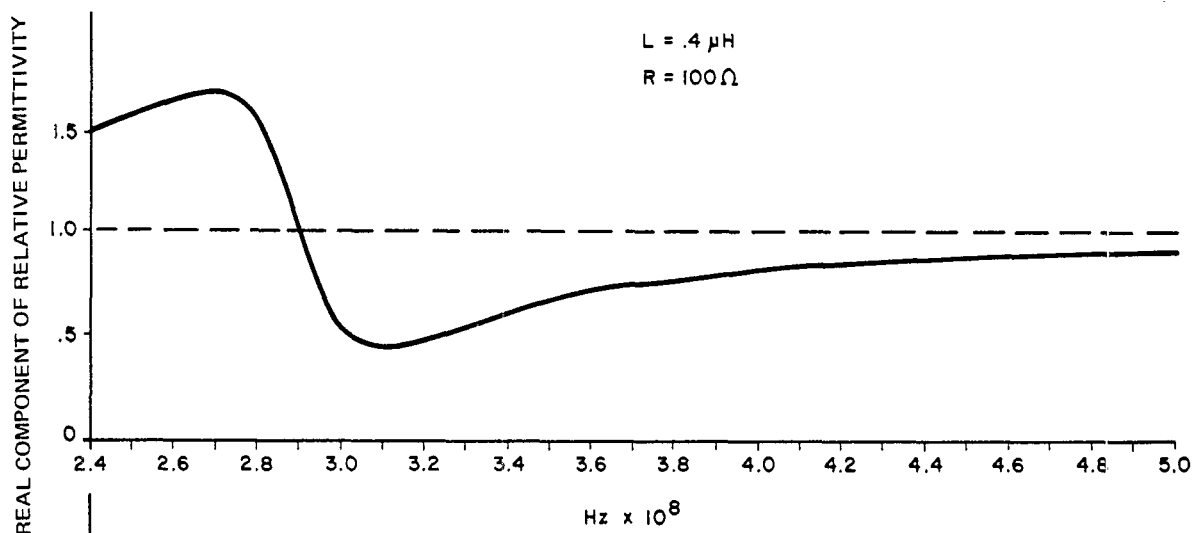


Figure 12c. The real component of relative permittivity calculated with equations (69) and (42). The value used for L is .4 μH and the value used for R is 100 Ω . The other parameters are the same as those employed to obtain figure 11.

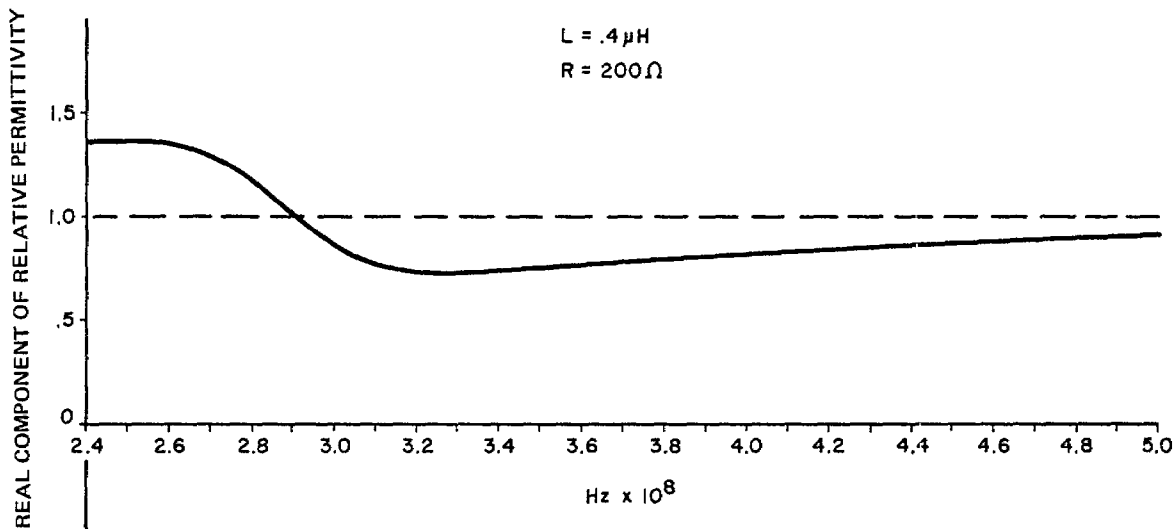


Figure 12d. The real component of relative permittivity calculated with equations (69) and (42). The value used for L is $.4 \mu\text{H}$ and the value used for R is 200Ω . The other parameters are the same as those employed to obtain figure 11.

In our first experiment we searched for the resonance predicted by equation (36) and shown in figure 12a. The experimental technique²⁵ was straightforward and is depicted in figure 13. The ratio of the incident electric field E_I to the reflected electric field E_R was obtained by measuring the standing wave ratio with a slotted line. The artificial dielectric sample shown in figure 13 consists of an aggregation of 48 of our 7 in. styrofoam balls each containing 3 mutually-perpendicular dipoles. The balls were enclosed in a rectangular box measuring 23 x 11.5 x 41.5 in. The results of the experiment are shown in figure 14. It is comforting to note that there is a large reflection at approximately the frequency of the resonance shown in figure 12a.

In a second series of experiments we measured the permittivity of our artificial dielectric utilizing the well-known shorted waveguide technique described in great detail by von Hippel²⁶. Very briefly, the technique consists of measuring the null point of a standing wave in a shorted waveguide. A sample of length l is then inserted into the shorted waveguide and the shift in the standing wave null is noted. The index of refraction of the dielectric sample of length l can then be calculated in terms of l and the shift in the standing wave null point.

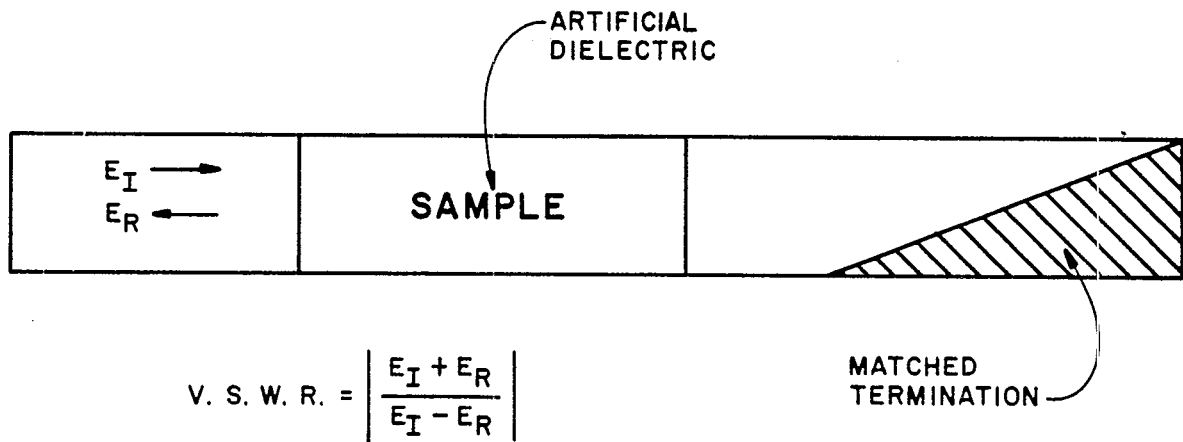


Figure 13. Experimental setup used in determining the resonance frequency of the artificial dielectric. The sample consisted of 48 scatterers or "molecules." The V.S.W.R. or voltage standing-wave ratio was determined with a slotted line.

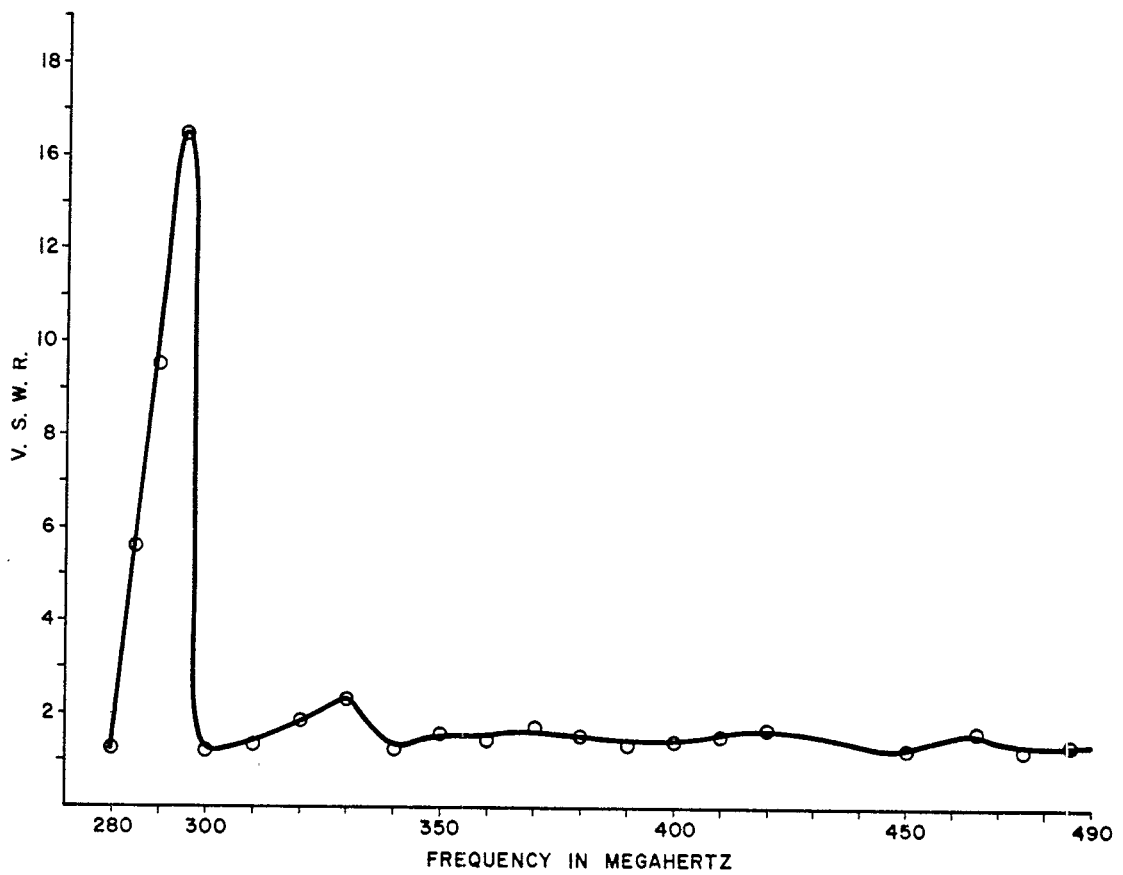


Figure 14. Experimental standing-wave ratio corresponding to the setup shown in figure 13.

Our experimental values of the index of refraction and some calculated values are shown in figure 15. The measurements were of two different artificial dielectric sample sizes; one sample consisted of an aggregation of 24 scatterers measuring 23 x 11.5 x 20.75 in. in volume. The length of the sample was, $\ell = 20.75$ in. The other sample consisted of an aggregation of 48 scatterers in a rectangular volume measuring 13 x 11.5 x 41.5 in. In this case, $\ell = 41.5$ in.

The difference between the theoretical index of refraction curve corresponding to $L = 0.4 \mu\text{H}$ and $R = 0$ and the measured index of refraction is about 30 percent. A possible source of the disparity between experiment and theory is that we used the dimension of the cardboard box that enclosed the scatterers to obtain ℓ . The effective length of the very granular artificial dielectric sample is most probably not the size of the box containing the scatterers. The boundary of our artificial dielectric is somewhat nebulous and needs more study.

Further experimental measurements of the electromagnetic characteristics of our inductively-loaded dipoles are now under consideration. These new measurements would involve the irradiation of a monopole that is immersed in an expanse of artificial dielectric medium. The new experimental approach would overcome the limitations imposed by the relatively small size and narrow frequency band pass of a waveguide. The measurements could also be carried out at lower frequencies which are closer to the actual nuclear EMP spectrum. As the frequency is lowered, the size of the scatterer compared to the wavelength would decrease. That is to say, the artificial dielectric would have less granularity and the boundary of the artificial dielectric would become more well defined.

If we construct a cylindrical monopole of height H it would have a resonance or maximum skin current at frequency f given by

$$f = \frac{4H}{\pi c}.$$

If the monopole were then submerged into an artificial dielectric with an index of refraction n , the resonance of the monopole would change to

$$f = \frac{4H}{\pi c} n.$$

The influence of the artificial dielectric of the resonance characteristics and skin currents of other shapes such as a sphere could also be studied.

COMPARISON OF EXPERIMENTAL
AND THEORETICAL VALUES OF
THE INDEX OF REFRACTION.

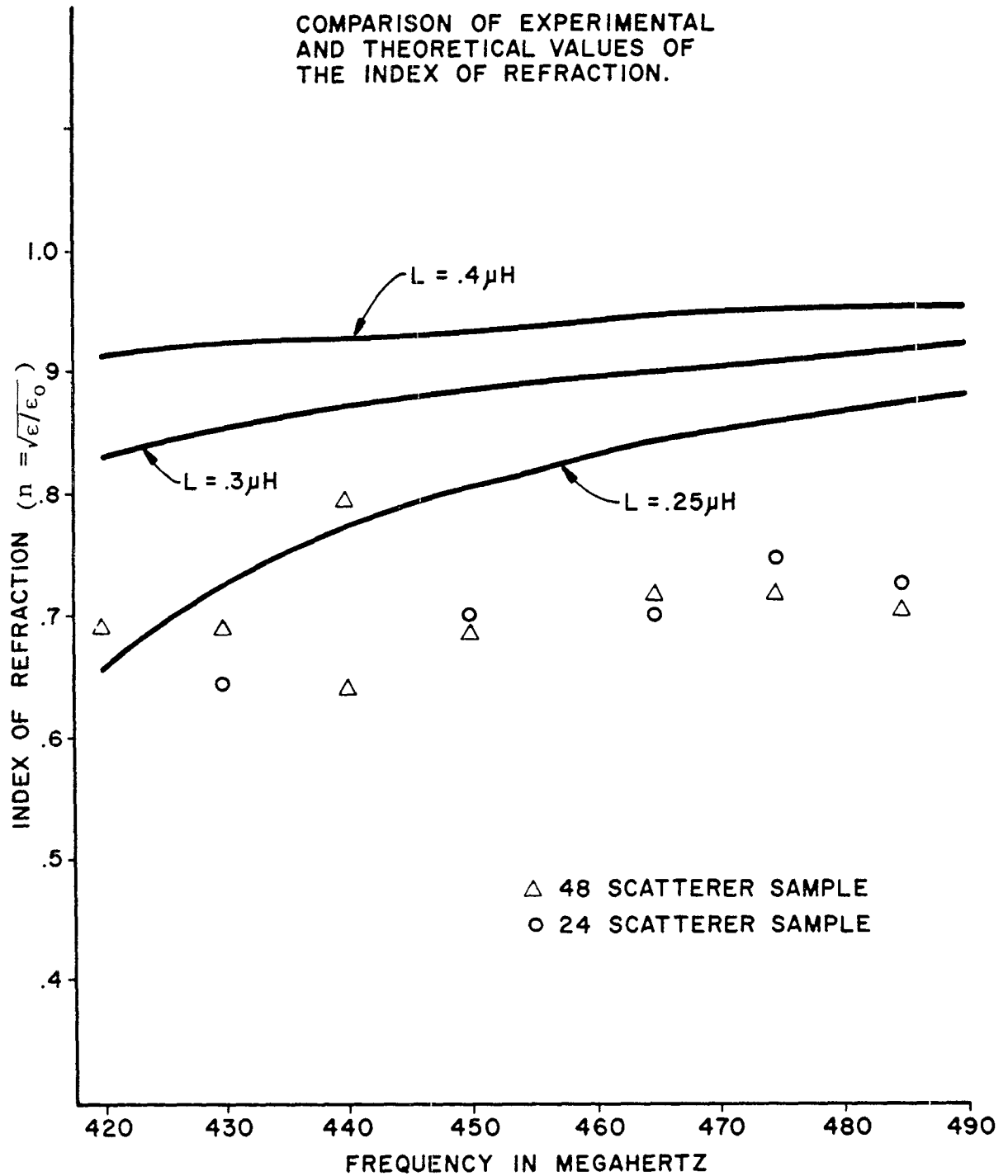


Figure 15. The accuracy of the experimental points is limited by the granularity of the sample and the corresponding indefiniteness of the sample edges.

4. SUMMARY AND CONCLUSIONS

We first introduced a simple quasi-static model of the artificial dielectric consisting of inductively-loaded dipoles which (1) ignored the dipole capacitance, and (2) assumed that the dipole-dipole interaction could be neglected. These two simplifying assumptions yielded an expression for the permittivity of the artificial dielectric that behaved in a manner surprisingly analogous to the permittivity of a simple Lorentzian plasma. It was noted that the granularity of fluctuations of the artificial dielectric could be decreased by constructing the dipole scatterers out of three mutually-perpendicular scatterers.

Then the effect of the capacitance of the inductively-loaded dipole scatterers was examined and limits set on the assumption that the inductance dominated the behavior of the inductively-loaded dipole. Next, the effect of dipole-dipole interactions on the artificial dielectric was considered. A relatively rigorous expression for a cubic, tetragonal or hexagonal lattice was obtained. An estimate of the effect of a random distribution of scatterers on the value of the permittivity predicted by equation (42) was also obtained.

It is interesting that the more exact expressions for the dielectric constant of the artificial dielectric, which considered both the effect of the capacitive dipole impedance and the dipole-dipole interaction, did not model the behavior of a Lorentzian plasma as well as the original simplified approach. Nevertheless, the artificial dielectric did have an index of refraction less than one over a relatively broad spectrum. We are now looking into the possibility of improving correspondence between the frequency dependence of our artificial dielectric and a Lorentzian plasma. The approach being investigated is based on the substitution of a more complicated one-terminal pair in place of the simple inductive dipole load used in our present scatterers. By synthesizing a suitable one-terminal pair out of a number of lumped impedances we hope to improve the correspondence between the frequency dependence of the artificial dielectric and a Lorentz plasma.

The experimental examination of the theoretical expressions for the dielectric constant of our artificial dielectric was constrained by the dimensions and frequency characteristics of available waveguide equipment. The predictions of equations (36) and (42) for the dielectric constant of the artificial dielectric were found to be in fair agreement with experimental results.

REFERENCES

1. M.A. Heald and C.B. Wharton, Plasma Diagnostics with Microwave, John Wiley and Sons, Inc., New York, 1965, p. 6.
2. W. Rotman, "Plasma Simulation by Artificial Dielectric and Parallel-plate Media," IRE Transactions on Antennas and Propagation, Vol. AP-13, p. 587, July 1965.
3. W.E. Koch, "Metallic Delay Lenses," Bell System Technical Journal, Vol. 27, pp. 58-82, January 1948.
4. J. Brown, "Microwave Lenses," Methuen and Co., Ltd., London, 1953.
5. H. Jasik, Antenna Engineering, McGraw-Hill Book Co., New York, 1963, Section 14.6. Schelkunoff and Friis, Antennas Theory and Practice, John Wiley and Sons, Inc., New York, 1952, p.577.
6. R.W. Corkum, "Isotropic Artificial Dielectrics," Proc. IRE, Vol. 40, pp. 574-587, May 1952.
7. M.M.Z. El-Kharadly and W. Jackson, "The Properties of Artificial Dielectrics Comprising Arrays of Conducting Particles," Proc. IEE (London), Vol. 100, Part III, pp. 199-212, July, 1953.
8. K.E. Golden, "Simulation of a Thin Plasma Sheath by a Plane of Wires," IRE Transactions on Antennas and Propagation, Vol. AP-13, p. 587, July 1965.
9. J. Brown, "Artificial Dielectrics Having Refractive Indices Less than Unity," Proc. IEE, Monograph No. 62R, Vol. 100, p. 51.
10. M.M.Z. El-Kharadly, "Some Experiments on Artificial Dielectrics at Centimetre Wavelengths," Proc. IEE, Paper No. 1700, Vol. 102B, p. 22, January 1955.
11. L. Brillouin, Wave Propagation in Periodic Structures, McGraw-Hill, New York, 1946.
12. J.C. Slater, Microwave Electronics, D. Van Nostrand Co., New York, 1950.
13. H.S. Bennett, "The Electromagnetic Transmission Characteristics of Two Dimensional Lattice Medium," J. Appl. Phys., Vol. 24, pp. 785-810, June 1953.
14. P.J. Crepeau and P.R. McIsaac, "Consequences of Symmetry in Periodic Structures," Proc. IEE, January 1964, p. 33.

15. R. F. Harrington, "Small Resonant Scatterers and Their Use for Field Measurements," IRE Transactions of Microwave Theory and Techniques, May 1962, pp. 165-174.
16. V.H. Ramsey, "The Reaction Concept in Electromagnetic Theory," Phys. Rev. Ser. 2, 94, No. 6, pp. 1483-1491, June 15, 1954.
17. R.F. Harrington, Time-Harmonic Electromagnetic Fields, McGraw-Hill Book Co., New York, 1961, Section 7-9.
18. R.W.P. King, The Theory of Linear Antennas, Harvard University Press, Cambridge, Mass., 1956, p. 184.
19. Ibid., p. 470.
20. R.W.P. King, R.B. Mack, and S.S. Sandler, Arrays of Cylindrical Dipoles, Harvard University Press, Cambridge, Mass., p. 359, Formula 8.87, 887.
21. J.H. Richmond, "Coupled Linear Antennas with Skew Orientation," IEEE Transactions on Antennas and Propagation, Vol. AP-18, No. 5, September 1970, pp. 694-696.
22. R.E. Collin, Field Theory of Guided Waves, McGraw-Hill Book Co., New York, 1960, p. 517.
23. J.G. Kirkwood, "On the Theory of Dielectric Polarization," J. Chem. Phys., Vol. 6, p. 592, September 1936.
24. J.G. Kirkwood, "The Local Field in Dielectrics," Annals of the New York Academy of Sciences, Vol. XL, Article 5, p. 315.
25. E.L. Ginston, Microwave Measurements, McGraw-Hill, New York, 1959, p. 235.
26. A.R. von Hippel, Editor, Dielectric Materials and Applications, The M.I.T. Press, Cambridge, Mass., 1954, Section 2, p. 63, by William B. Westphal.

DISTRIBUTION

DIRECTOR
DEFENSE ADVANCED RESEARCH PROJECTS AGENCY
ARCHITECT BUILDING
1400 WILSON BLVD
ARLINGTON, VIRGINIA 22209
ATTN DIR, TECH INFO, F.A. KOETHER

COMMANDER IN CHIEF
CONTINENTAL AIR DEFENSE COMMAND
ENT AFD
COLORADO SPRINGS, COLORADO 80912
ATTN DCS/C+E (CESA), DR. J.K. STERRETT
ATTN CPPA DR W R MATOUSH

ASSISTANT TO THE SECRETARY OF DEFENSE
TELECOMMUNICATIONS
WASHINGTON DC 20103
ATTN OPERATIONS + ENGINEERING

DEFENSE CIVIL PREPAREDNESS AGENCY
WASHINGTON DC 20301
ATTN TS(AED) RM IC 535
ATTN REISS, H E ROEDERICK
ATTN G VANDENBERGHE RM IE 542

DIRECTOR
DEFENSE COMMUNICATIONS AGENCY
WASHINGTON, D.C. 20305
ATTN CODE 350, J A KRCEK
ATTN CODE 340, W.H. DIX
ATTN CODE 931
ATTN CODE 8210, WPN SYS ANAL DIV
ATTN CODE 320.4
ATTN CODE 950
ATTN CODE 400

NATIONAL COMMUNICATION SYSTEM
OFFICE OF THE MANAGER
WASHINGTON DC 20305
ATTN NCS-DE DENNIS BODSON

DEFENSE COMMUNICATION ENGINEERING OFFICE
1860 WIEHLE AVENUE
RESTON VIRGINIA 22070
ATTN H620

DEFENSE DOCUMENTATION CENTER
CAMERO STATION, BUILDING 5
ALEXANDRIA, VIRGINIA 22314
ATTN DDC-TCA 12 COPIES

DIRECTOR
DEFENSE INTELLIGENCE AGENCY
WASHINGTON, D.C. 20301
ATTN DI-76, PHYS VUL DIV, E O'FARRELL

DIRECTOR
DEFENSE NUCLEAR AGENCY
WASHINGTON, D.C. 20305
ATTN STRA, RADIATION DIRECTORATE
ATTN RAEV, ELECTRONICS VULNERABILITY
DIVISION
ATTN APIL, DASA TECH LIBRARY 2 COPIES
ATTN STVL, VULNERABILITY DIRECTORATE
ATTN DDST, SCIENTIFIC ASST, P. HAAS
ATTN APSI (ARCHIVES)

COMMANDER
FIELD COMMAND
DEFENSE NUCLEAR AGENCY
KIRTLAND AFB, NEW MEXICO 87115
ATTN FCTA-A TECHNICAL LIBRARY

CHIEF
LIVERMORE DIVISION, FIELD COMMAND, DNA
LAWRENCE LIVERMORE LABORATORY
P.O. BOX 808
LIVERMORE, CALIFORNIA 94550
ATTN DOCUMENT CONTROL

DIRECTOR OF DEFENSE RES AND ENGINEERING
WASHINGTON, D.C. 20301
ATTN SPECIAL ASST (NET TECH ASSES)
N.F. WIKNER
ATTN DEP DIR (STRATEGIC SYSTEMS)
ATTN ASST DIR (ELECT+PHYS SCI)
G.H. HEILMEIER

CHAIRMAN
JOINT CHIEFS OF STAFF
WASHINGTON, D.C. 20301
ATTN J-5, PLANS AND POLICY
(R AND D DIVISION)
ATTN J-6, CSD-1
ATTN J6 LCOL LOGSDEN

DIRECTOR
JOINT STRAT TARGET PLANNING STAFF
OFFUTT AFB
OMAHA, NEBRASKA 68113
ATTN JLTW
ATTN JPST

CHIEF
NATIONAL MILITARY COMMAND SYS SUP CENTER
THE PENTAGON
WASHINGTON, D.C. 20301
ATTN B210 RM BE 685

DIRECTOR
NATIONAL SECURITY AGENCY
FORT GEORGE G. MEADE, MARYLAND 20755
ATTN O. D. VAN GUNTEN, R-425
ATTN TOL
ATTN S06 KEN EDWARDS

HEADQUARTERS
EUROPEAN COMMAND
J-5
APO NEW YORK, NEW YORK 09128
ATTN ECJE-WP

HEADQUARTERS
US EUROPEAN COMMAND (S-6)
APO NEW YORK, NEW YORK 09055
ATTN ECCE-PT

COMMANDER-IN-CHIEF
PACIFIC COMMAND
FPO SAN FRANCISCO, CALIFORNIA 96610
ATTN J305

DIRECTOR
WEAPONS SYSTEMS EVAL GROUP, ODDRE
OFFICE, SECRETARY OF DEFENSE
400 ARMY-NAVY DRIVE
WASHINGTON, D.C. 20305
ATTN CAPT DONALD E. MCCOY, USN
ATTN H.A. KNAPP, JR.

COMMANDER
AARDCOM (ARMY AIR DEFENSE COMMAND)
ENT AFD
COLORADO SPRINGS, COLORADO 80912
ATTN ADGP, W BARNES
ATTN ADGPA

OFFICE OF THE SECRETARY OF THE ARMY
WASHINGTON DC 20310
ATTN OUSA (OR) DR DANIEL WILLARD

ASSISTANT CHIEF OF STAFF FOR
COMMUNICATIONS-ELECTRONICS
DEPARTMENT OF THE ARMY
WASHINGTON, D.C. 20314
ATTN CEED-7, WESLEY T. HEATH

ASSISTANT CHIEF OF STAFF FOR INTELLIGENCE
DEPARTMENT OF THE ARMY
WASHINGTON, D.C. 20310
ATTN MITA/OM LIBRARY

COMMANDER-IN-CHIEF
USA EUROPE AND 7TH ARMY HQ
APO NEW YORK, NEW YORK 09403
ATTN AEAGE-T2
ATTN DDSC-E, AEAGE-PI

OFFICE, CHIEF OF RESEARCH + DEVELOPMENT
DEPARTMENT OF THE ARMY
WASHINGTON, D.C. 20310
ATTN DARD-HDD, LTC H. SLOAN
ATTN DARD-UDM-W, MAJ B GRIGGS
ATTN ABRDA-00

COMMANDER
USA ADVANCED BALLISTIC MISSILE DEF AGENCY
HUNTSVILLE OFFICE
P. O. BOX 1500
HUNTSVILLE, ALABAMA 35807
ATTN RDMH-D
ATTN RDMH-X
ATTN CRDAH-S, ROLAND BROWN

COMMANDER
USA SAFEGUARD COMMUNICATIONS AGENCY
ATTN DOCUMENT CONTROL
FORT HUACHUCA, ARIZONA 85613
ATTN SPECIAL SCIENTIFIC ACTIVITIES DIR

SAFEGUARD SYSTEM MANAGER
USA SAFEGUARD SYSTEM OFFICE
COMMONWEALTH BUILDING
1320 WILSON BLVD.
ARLINGTON, VIRGINIA 22209
ATTN REENTRY PHYSICS, J.J. SHEA
ATTN RES + ENG, MAJ TEALE, DAC-SAE-S

COMMANDER
SAFEGUARD SYSTEM SITE ACTIVATION COMMAND
GRAND FORKS
P O BOX 631
LANGDON, NORTH DAKOTA 58249
ATTN DEP FOR SITE ACTIVATION

COMMANDER
USA SAFEGUARD SYSTEMS COMMAND
P. O. BOX 1500
HUNTSVILLE, ALABAMA 35807
ATTN SSC-STP, J H DAUGHTRY
ATTN SSC STE
ATTN SSC-DEM
ATTN SSC-DEM, L L DICKERSON
ATTN SSC-DH

COMMANDER
USA SAFEGUARD SYSTEMS COMMAND
FIELD OFFICE
BELL TELEPHONE LABORATORIES
WHIPPANY ROAD
WHIPPANY, NEW JERSEY 07981
ATTN SSC-DEF-B, J TURNER
SAFCOM PROJ ENGINEER

COMMANDER
USA SAFEGUARDS SYSTEM EVALUATION AGENCY
WHITE SANDS MISSILE RANGE, NM 88002
ATTN SAFSEA-EAB
ATTN SSEA-RB

COMMANDER
HQ, US ARMY MATERIEL COMMAND
5001 EISENHOWER AVENUE
ALEXANDRIA, VIRGINIA 22304
ATTN AMCDL, DEP FOR LABORATORIES
ATTN AMCRD, DIR RES, DEV & ENGR
ATTN AMCRD-WN, JOHN CORRIGAN
ATTN AMCHS-IS, ALDAIC SAUCIER

COMMANDER
US ARMY MATERIEL COMMAND
REDSTONE ARSENAL, ALABAMA 35809
ATTN AMCPM-LGES, H HENDRICKSON
ATTN AMCPM-MD, SAM-D PROJ DFC
ATTN AMCPM-MDE
ATTN AMCPM-MDE, MAJ STANLEY

COMMANDER
US ARMY MATERIEL COMMAND
FORT MONMOUTH, NEW JERSEY 07703
ATTN AMCPM-TDS, PROJ MGR, ARMY TACTICAL
DATA SYSTEMS (ARTADS)
ATTN AMCPM-TDS-TF

COMMANDER
USA COMMUNICATIONS SYSTEMS AGENCY
FORT MONMOUTH, NEW JERSEY 07703
ATTN LIBRARY
ATTN SEYMOUR KREVSKEY, DEP DIR ENGR

COMMANDER
ARMY MATERIALS & MECHANICS RESEARCH CENTER
WATERLOO, MASSACHUSETTS 02172
ATTN AMXMR-XH, JOHN DIGNAN

COMMANDER
USA FOREIGN SCIENCE & TECHNOLOGY CENTER
FEDERAL OFFICE BUILDING
220 7TH STREET N.E.
CHARLOTTEVILLE, VIRGINIA 22901
ATTN AMXST-IDI DR P A CROWLEY
ATTN AMXST-ISI D MC CALLUM
ATTN LIBRARY SERVICES BRANCH

COMMANDER
USA SATELLITE COMMUNICATIONS AGENCY
FORT MONMOUTH, NEW JERSEY 07703
ATTN AMCPM-SC-6, MR PERLE

COMMANDER
USAMC ABERDEEN RESEARCH & DEV CENTER
ABERDEEN PROVING GROUND, MARYLAND 21005
ATTN AMXRD-BVL, J.W. MC NEILLY
ATTN AMXRD-BVL, J.W. KINCH

COMMANDER
USA ELECTRONICS COMMAND
FORT MONMOUTH, NEW JERSEY 07703
ATTN AMSEL-TL-NN, DR E HOTH
ATTN AMSEL-TL-ND, E.T. HUNTER
ATTN AMSEL-TL-D, H K ZIEGLER
ATTN AMSEL-GG-TD, SARAH DWANSON
ATTN AMSEL-NL-E-S, HILT LIPTON
ATTN AMSEL-NL-D
ATTN AMSEL-TL-D
ATTN AMSEL-TL-ME, M POMERANTZ
ATTN AMSEL-GG-M, G K GAULE
ATTN AMSEL-TL-NR, DR H A BOMKE
ATTN AMSEL-WL-D
ATTN AMSEL-CT-MDX, COHEN
ATTN AMSEL-TL-N, DR S KRONENBERG
ATTN AMSEL-TL-NS, R FREIBERG

COMMANDER
USA ELECTRONICS COMMAND
FORT BELVOIR, VIRGINIA 22060
ATTN AMSEL-NV, CPT PARKER

COMMANDER
USA MISSILE COMMAND
REDSTONE ARSENAL, ALABAMA 35809
ATTN AMSMI-RBLD, CHIEF DOC SECTION
ATTN AMCPM-HA, HAWK PROJ DFC
ATTN AMSMI-RGG, J. HOLEMAN
ATTN AMSMI-RV, MR. LIVELY
ATTN AMCPM-PE-EA, S D COZBY

COMMANDER
USA MOBILITY EQUIPMENT R & D CENTER
FORT BELVOIR, VIRGINIA 22060
ATTN SMEFB-MM, J W BOND
ATTN SMEFB-BA, R K YOUNG
ATTN SMEFB-RN, D B DINGER
ATTN T W OCONNOR, JR
ATTN SMEFB-MHD, F P GOOD
ATTN SMEFB-XN, W J HAAS
ATTN SMEFB-ES, R S BRANTLY, JR

COMMANDER
USA MUNITIONS COMMAND
DOVER, NEW JERSEY 07801
ATTN AMSMU-RE-CN, SYS DEV DIV,
CHEMICAL & NUCLEAR
MR WAXLER

COMMANDER
PICATINNY ARSENAL
DOVER, NEW JERSEY 07801
ATTN SHUPA-FR-E, L AVRAMI
ATTN SHUPA-FR-S
ATTN SHUPA-TS-T-S, TECHNICAL LIBRARY
ATTN SHUPA-ND, P. ZIRKIND
ATTN SHUPA-ND-ME
ATTN SHUPA-ND-C-S DR AMINO NORDIO
ATTN SHUPA-ND-DC2
ATTN SHUPA-ND-DB, E J ARBER
ATTN SHUPA-ND-DA3
ATTN SHUPA-NDB 300, BLOG 95,
ARTHUR NICHOLS
ATTN SHUPA-RT-S, FOR JANTIP
ATTN SHUPA-ND-W
ATTN SHUPA-OA-M, P G OLIVIERI
ATTN SHUPA-TS-I-E, A GRINGOCH
ATTN HYMAN POSTERNAK

COMMANDER
USA TEST & EVALUATION COMMAND
ABERDEEN PROVING GROUND, MD 21005
ATTN AMSTE-EL, R.L. KOLCHIN
ATTN AMSTE-NB, R.R. GALASSO

COMMANDER
USA ABERDEEN PROVING GROUND
ABERDEEN PROVING GROUND, MARYLAND 21005
ATTN STEAP-TL, USAARDC BR (DRL) BLD 330

PRESIDENT
USA AIRBORNE COMMUNICATIONS & ELECT BD
FORT BRAGG, NORTH CAROLINA 28307
ATTN STEB-MA-A

COMMANDER
USA ELECTRONICS PROVING GROUND
FORT HUACHUCA, ARIZONA 85613
ATTN STEEP-MT-G
ATTN STEEP-MT-M, MR MCINTOSH

COMMANDER
WHITE SANDS MISSILE RANGE, NM 88002
ATTN STEWS-TE-N, M.P. SQUIRES

COMMANDER
USACDC NUCLEAR AGENCY
FORT BLISS, TEXAS 79916
ATTN CDCNA-E

COMMANDER
USACDC ARMOR AGENCY
FORT KNOX, KENTUCKY 40121
ATTN DOCUMENT CONTROL

COMMANDER
USACDC COMMUNICATIONS-ELECTRONICS AGENCY
FORT MONMOUTH, NEW JERSEY 07703
ATTN CHIEF, M/E DIV

COMMANDER
USA COMPUTER SYSTEMS COMMAND
FORT BELVOIR, VA 22060
ATTN CSCS-EME-E, E T PARKER
ATTN CSCS-EME-C

CHIEF OF ENGINEERS
DEPARTMENT OF THE ARMY
WASHINGTON, D.C. 20314
ATTN DAEN-MCE-D, MR MC CALLEY

DIVISION ENGINEER
USA ENGINEER DIVISION, MISSOURI RIVER
P.O. BOX 103 DOWNTOWN STATION
OMAHA, NEBRASKA 68101
ATTN MREDE-MC, F L HAZLETY,
SPEC PROJ COORDINATOR

COMMANDER
ARMY NUCLEAR & CHEMICAL SURETY GROUP
FORT BELVOIR, VIRGINIA 22060
ATTN FDSG-ND, BLOG 2073, NORTH AREA

COMMANDER
US ARMY SECURITY AGENCY
ARLINGTON HALL STATION
ARLINGTON, VA 22212
ATTN IARD-EL
ATTN SPECIAL PROJECTS ELEMENT

COMMANDER
USA STRATEGIC COMMUNICATIONS COMMAND
FORT HUACHUCA, ARIZONA 85613
ATTN SCCX-SSA-00
ATTN SCCX-SSA, COL H J STIRLING

COMMANDER
USA COMMAND & GENERAL STAFF COLLEGE
FORT LEAVENWORTH, KANSAS 66027
ATTN ATSCS-SE-L

COMMANDER
USA FIELD ARTILLERY SCHOOL
FORT SILL, OKLAHOMA 73503
ATTN ATSPA-CA-NM

CHIEF OF NAVAL OPERATIONS
NAVY DEPARTMENT
WASHINGTON, D.C. 20350
ATTN NOP-985F2, CDR S.I. STOCKING
ATTN NOP-932
ATTN NOP-03EG

CHIEF OF NAVAL RESEARCH
DEPARTMENT OF THE NAVY
ARLINGTON, VIRGINIA 22217
ATTN DNR-427
ATTN DNR-418, G.R. JOINER

COMMANDER
NAVAL AIR SYSTEMS COMMAND, HQ
1411 JEFFERSON DAVIS HIGHWAY
ARLINGTON, VIRGINIA 20360
ATTN LCDR HUGO HARDT AIR-350-F

COMMANDING OFFICER
NAVAL AMMUNITION DEPOT
CRANE, INDIANA 47522
ATTN CODE 7024, JAMES L. RAMSEY

COMMANDING OFFICER
NAVAL CIVIL ENGINEERING LABORATORY
PORT HUENEME, CALIFORNIA 93043
ATTN CODE L31

COMMANDER
NAVAL COMMUNICATIONS COMMAND HQ
4401 MASSACHUSETTS AVE, N.W.
WASHINGTON, D.C. 20390
ATTN N-7, LCDR HALL

COMMANDER
NAVAL ELECTRONICS SYSTEMS COMMAND, HQ
2511 JEFFERSON DAVIS HIGHWAY
ARLINGTON, VIRGINIA 20360
ATTN NELEX-05123
ATTN NELEX-5124, BERT FOX
ATTN NELEX-0518

COMMANDER
NAVAL ELECTRONICS LABORATORY CENTER
SAN DIEGO, CALIFORNIA 92152
ATTN TECHNICAL LIBRARY
ATTN CODE 3100, E.E. MC COWN
ATTN CODE 3200, H.F. WONG

COMMANDER
NAVAL INTELLIGENCE SUPPORT CENTER
4301 SUITLAND ROAD
WASHINGTON, D.C. 20390
ATTN DR P ALEXANDER
ATTN NISC-41

COMMANDER
NAVAL ORDNANCE LABORATORY
WHITE OAK, MARYLAND 20910
ATTN CODE 121, NUCLEAR PROGRAM OFC
ATTN CODE 244, EXPLOSIONS EFFECTIVENESS
DIVISION
ATTN CODE 730, LIBRARY DIVISION
ATTN CODE 431, NORMAN TASLITT
ATTN DR M C PETREE
ATTN R A SMITH
ATTN E R RATHBUN

6 COPIES

COMMANDER
NAVAL ORDNANCE SYSTEMS COMMAND, HQ
2521 JEFFERSON DAVIS HIGHWAY
ARLINGTON, VIRGINIA 20360
ATTN NORD-0523, R. LANE

SUPERINTENDENT
NAVAL POSTGRADUATE SCHOOL
MONTEREY, CALIFORNIA 93940
ATTN CODE 2124, LIBRARY

DIRECTOR
NAVAL RESEARCH LABORATORY
WASHINGTON, D.C. 20390
ATTN CODE 4004, E. L. BRANCATO
ATTN CODE 6465, DR. RICHARD L. STATLER
ATTN CODE 7001, J.O. BROWN

COMMANDING OFFICER
NAVAL SCIENTIFIC AND TECHNICAL
INTELLIGENCE CENTER
4301 SUITLAND ROAD, BLOG 5
WASHINGTON, D.C. 20390
ATTN DOCUMENT CONTROL

COMMANDER
NAVAL SHIP ENGINEERING CENTER
3700 E-ST-WEST HIGHWAY
PRINCE GEORGES PLAZA
HYATTSVILLE, MARYLAND 20782
ATTN NSEC-6174D2, EDWARD F. DUFFY
ATTN NSEC-6015C, EDWARD BERKOWITZ

COMMANDER
NAVAL SHIP SYSTEMS COMMAND, HQ
2531 JEFFERSON DAVIS HIGHWAY
WASHINGTON, D.C. 20360

COMMANDER
NAVAL UNDERSEA CENTER
SAN DIEGO, CALIFORNIA 92132
ATTN CODE 608, C F RAMSTEDT

COMMANDER
NAVAL WEAPONS CENTER
CHINA LAKE, CALIFORNIA 93555
ATTN CODE 753, LIBRARY DIVISION

NAVAL WEAPONS ENGINEERING SUPPLY ACTVY
WASHINGTON NAVY YARD
WASHINGTON, DC 20390
ATTN E, S, A, 70

COMMANDING OFFICER
NAVAL WEAPONS EVALUATION FACILITY
KIATLAND AFB, NEW MEXICO 87117
ATTN CODE WE, MR. STANLEY
ATTN L OLIVER

COMMANDER
NAVAL WEAPONS LABORATORY
DAHLGREN, VIRGINIA 22448
ATTN WILLIAM H. HOLT

COMMANDING OFFICER
NAVAL WEAPONS STATION
CONCORD, CALIFORNIA 94520
ATTN QUAL EVAL LAB, CODE 33120,
DR. ROBERT WAGNER

COMMANDER
NAVY ASTRONAUTICS GROUP
POINT MUGO, CALIFORNIA 93042
ATTN WILLIAM GLEESON

COMMANDING OFFICER
NAVY SPACE SYSTEM ACTIVITY
BOX 92960
WORLDWAYS POSTAL CENTER
LOS ANGELES CALIF 90009
ATTN DR E E MUEHLNER

COMMANDER
NUCLEAR WEAPONS TRAINING CTR, PACIFIC
NAVAL AIR STATION, NORTH ISLAND
SAN DIEGO, CALIFORNIA 92135
ATTN CODE 52

COMMANDER
NUCLEAR WEAPONS TRAINING GROUND, ATLANTIC
NORFOLK, VIRGINIA 23511
ATTN DOCUMENT CONTROL

DIRECTOR
STRATEGIC SYSTEMS PROJECTS OFFICE
NAVY DEPARTMENT
WASHINGTON, D.C. 20390
ATTN NSP-431, TECHNICAL LIBRARY
ATTN NSP-230, DAVID GOLD
ATTN NSP-2342, R.L. COLEMAN
ATTN NSP-2701, JOHN W. PITSEMBERGER
ATTN NSP-273, PHIL SPECTOR
ATTN NSP-2701, CDR L STOESSL

COMMANDER-IN-CHIEF
US ATLANTIC FLEET
NORFOLK, VIRGINIA 23511
ATTN DOCUMENT CONTROL

COMMANDER-IN-CHIEF
US PACIFIC FLEET
FPO SAN FRANCISCO 96610
ATTN DOCUMENT CONTROL(303)

CHIEF OF STAFF
US AIR FORCE, HQ
WASHINGTON, D.C. 20330
ATTN RDOPN
IS/V + NUCLEAR PROGRAMS DIV.)
ATTN PRCCS, LTC WOODRUFF
ATTN RDPS, MR PORTER
ATTN IGSPB, ED CALVERT

COMMANDER
AEROSPACE DEFENSE COMMAND
ENT AFB, COLORADO 80912
ATTN XPDW, ADVANCED PLANNING DIV.
ATTN DEEDS, J C. BRANNAN

COMMANDER
AIR UNIVERSITY
MAXWELL AFB, ALABAMA 36112
ATTN AUL/LSE-70-250

COMMANDER
HQ AIR FORCE SYSTEMS COMMAND
ANDREWS AFB
WASHINGTON, D.C. 20331
ATTN DLSP (GENERAL PHYSICS)

COMMANDER
AF AERO PROPULSION LABORATORY, AFSC
WRIGHT-PATTERSON AFB, OHIO 45433
ATTN P E STOVER

COMMANDER
AEROSPACE RESEARCH LABORATORIES, AFSC
WRIGHT PATTERSON AFB, OHIO 45433
ATTN CA
ATTN LS, DONALD C REYNOLDS

COMMANDER
AF AVIONICS LABORATORY, AFSC
WRIGHT-PATTERSON AFB, OHIO 45433
ATTN AAA, AVIONICS SYNTHESIS + ANAL BR
ATTN NVS, EUGENE C. MAUPIN
ATTN NVS, R CONKLIN
ATTN TEA, DR HANS HENNECKE

COMMANDER
AF WEAPONS LABORATORY, AFSC
KIRTLAND AFB, NEW MEXICO 87117
ATTN ELT, MAJ WALKER
ATTN SAA
ATTN SAB
ATTN SAY
ATTN EL, CAPT CARL DAVIS
ATTN EL, J DARRAH
ATTN ELE/EMP BRANCH
ATTN DOUL, TECHNICAL LIBRARY
ATTN ELE DR CARL BAUM

COMMANDER
ROME AIR DEVELOPMENT CENTER, AFSC
GRIFFISS AFB, NEW YORK 13440
ATTN RCRP, J.S. SMITH
ATTN TSGC
ATTN RCRN, CAPT R. BELLEN

COMMANDER
ARMAMENT DEVELOPMENT AND TEST CENTER
EGLIN AIR FORCE BASE, FLA. 32542
ATTN ADTC(DOCSL), TECH LIBRARY

COMMANDER
AERONAUTICAL SYSTEMS DIVISION, AFSC
WRIGHT-PATTERSON AFB, OHIO 45433
ATTN ASD/YH-EX, CAPT BRANHAM
ATTN ASD/ENVCB, ROBERT L. FISH
ATTN ASD/ENVED

COMMANDER
ELECTRONIC SYSTEMS DIVISION, AFSC
L. G. HANSCOM FIELD
BEDFORD, MASSACHUSETTS 01730
ATTN MCAE LTC DAVID SPARKS
ATTN XRE, SURVIVABILITY
ATTN LCD
ATTN YWES
ATTN DCKE
ATTN XRP/ MAJ GINGRICH
ATTN IN
ATTN DCD
ATTN MCL

COMMANDER
FOREIGN TECHNOLOGY DIVISION, AFSC
WRIGHT-PATTERSON AFB, OHIO 45433
ATTN PDIN, BALLARD
ATTN FTD/POJC

COMMANDER
HQ SPACE AND MISSILE SYSTEMS ORGANIZATION
P O 96960 WORLDWAYS POSTAL CENTER
LOS ANGELES, CALIFORNIA 90009
ATTN RSS SYSTEM ENGINEERING
ATTN SKD
ATTN SKE, DIR OF ENGR GP 1
ATTN SKT
ATTN IND, I J JUDY
ATTN XRT, STRATEGIC SYSTEMS DIV
ATTN SYJ, AEROSPACE DEFENSE PROG OFC
ATTN SZH, CAPT MARION F SCHNEIDER
ATTN SZJ, CAPT E.T. DEJONCKHEERE, JR.
ATTN GCD, CAPT A. MENDEKE JR.
ATTN DYS, MAJ HEILMAN
ATTN RSP SYSTEM DEFN+ ASSESSMENT
LTC GILBERT
ATTN OYJ, CAPT RASMUSSEN
ATTN RNF, MAJ COX

SPACE + MISSILE SYSTEMS ORGANIZATION
MCRTON AFB, CALIFORNIA 92409
ATTN SYGN, CAPT STRUBEL
ATTN RSTA, E A MERRITT

AF INSTITUTE OF TECHNOLOGY, AU
WRIGHT-PATTERSON AFB, OHIO 45433
ATTN AFIT(ENP)
DR. CHARLES J. BRIDGMAN.

HEADQUARTERS
AIRFORCE TECHNICAL APPLICATIONS CENTER
PATRICK AFB, FLORIDA 32925
ATTN TD-5B
ATTN TD-3

COMMANDER
STRATEGIC AIR COMMAND
OFFUTT AFB, NEBRASKA 68113
ATTN NRI/STINFO LIBRARY
ATTN NRW

US ATOMIC ENERGY COMMISSION
WASHINGTON, D. C. 20545
ATTN DIVISION OF HQ SERVICES
LIBRARY BRANCH, RALPH SHULL, DNA
ATTN: DNA, DOCUMENT CONTROL FOR
R+D BRANCH

US ATOMIC ENERGY COMMISSION
ALBUQUERQUE OPERATIONS OFFICE
P.O. BOX 5400
ALBUQUERQUE, NEW MEXICO 87115
ATTN DOCUMENT CONTROL

ADMINISTRATOR
DEFENSE ELECTRIC POWER ADMINISTRATION
DEPT OF INTERIOR
WASHINGTON DC 20204
ATTN IRVING I RAINES ROOM 5400

DEPARTMENT OF COMMERCE
NATIONAL BUREAU OF STANDARDS
WASHINGTON, D. C. 20234
ATTN ELECTRON DEV SECT, J.C. FRENCH

NATIONAL ACADEMY OF SCIENCES
2101 CONSTITUTION AVE NW
WASHINGTON DC 20418
ATTN DR R S SHANE
NATIONAL MATERIALS ADVISORY BOARD

NASA HEADQUARTERS
WASHINGTON, D. C. 20546
ATTN CODE REE, GUIDANCE, CONTROL
AND INFORMATION SYSTEMS

ARMS CONTROL AND DISARMAMENT AGENCY
REFERENCE INFORMATION CENTER
DEPARTMENT OF STATE
2201 C STREET, N.W.
WASHINGTON, DC 20451
ATTN CRSC/L AUDREY E EDMONDS

FEDERAL AVIATION ADMINISTRATION
DEPARTMENT OF TRANSPORTATION
800 INDEPENDENCE AVENUE, S.W.
WASHINGTON, D.C. 20590
ATTN F S SAKATE, RD 650

UNIVERSITY OF CALIFORNIA
LAWRENCE LIVERMORE LABORATORY
TECHNICAL INFORMATION DIVISION
P. O. BOX 808
LIVERMORE, CALIFORNIA 94551
ATTN L-48, DR. LOUIS F. HOUTERS
ATTN L-3, TECHNICAL INFO DEPT
ATTN L-31, WILLIAM J. HOGAN
ATTN L-24, HANS KRUGER
ATTN L-24, DR. DAVID OAKLEY
ATTN L-154, L L CLELAND
ATTN L-71, DR. W. GRAYSON
ATTN L-156 E K MILLER

UNIVERSITY OF CALIFORNIA
LAWRENCE RADIATION LABORATORY
LIBRARY, BUILDING 50, RM 134
BERKLEY, CALIFORNIA 94720
ATTN PROF KENNETH H. WATSON

UNIVERSITY OF CALIFORNIA
ATTN DOCUMENT CONTROL
LCS ALAMOS SCIENTIFIC LABORATORY
P.O. BOX 1663
LCS ALAMOS, NEW MEXICO 87544
ATTN GMX-T, TERRY R. GIBBS
ATTN DR. JOHN S. MALIK
ATTN J-DOT FOR DR RALPH PARTRIDGE
ATTN R.F. TASCHEK
ATTN J ARTHUR FREED

UNIVERSITY OF DENVER
COLORADO SEMINARY
DENVER RESEARCH INSTITUTE
ATTN SECURITY OFFICER
P.O. BOX 10127
DENVER, COLORADO 80210
ATTN FRED P VENOITTI
ATTN R.W. BUCHANAN

GEORGIA INSTITUTE OF TECHNOLOGY
OFFICE OF RESEARCH ADMINISTRATION
ATLANTA, GEORGIA 30332
ATTN RES + SFC COORD FOR H DENNY

IIT RESEARCH INSTITUTE
10 WEST 35TH STREET
CHICAGO, ILLINOIS 60616
ATTN J.E. BRIDGES, ENGR ADVISOR
ATTN J.J. KRSTANSKY, ASST DIR OF RSCH
ATTN I.M. MINDEL

IIT RESEARCH INSTITUTE
ELECTROMAGNETIC COMPATIBILITY ANALYSIS
CENTER
NORTH SEVERN-ECAC BLDG.
ANNAPOLIS, MARYLAND 21402
ATTN ACDAT

MIT LINCOLN LABORATORY
P.O. BOX 73 / 244 WOOD STREET
LEXINGTON, MASSACHUSETTS 02173
ATTN ALAN G. STANLEY

C.S. DRAPER LABORATORY DIVISION OF
MASSACHUSETTS INSTITUTE OF TECHNOLOGY
224 ALBANY STREET
CAMBRIDGE MASSACHUSETTS 02139
ATTN KEVIN FERTIG, MS-87

TEXAS TECH UNIVERSITY
P O BOX 5404 NURTH COLLEGE STA
LURBOCK, TEXAS 79409
ATTN TRAVIS L SIMPSON

AEROJET ELECTRO-SYSTEMS CO. DIV.
AEROJET-GENERAL CORPORATION
P.O. BOX 296
AZUSA, CALIFORNIA 91702
ATTN T.O. HANSCOME, 6181/170
ATTN R.Y. KAKUDA, B-194/D-6121

AEROJET ENERGY CONVERSION COMPANY
AEROJET LIQUID ROCKET COMPANY
P.O. BOX 13222
SACRAMENTO, CALIFORNIA 95813
ATTN DEPT 8130

AEROJET ENERGY CONVERSION COMPANY
AEROJET NUCLEAR SYSTEMS COMPANY
P.O. BOX 13070
SACRAMENTO, CALIFORNIA 95813
ATTN TECH LIB, DEPT N4264, BLDG 2019A1

AEROSPACE CORPORATION
P O BOX 92957
LOS ANGELES, CALIFORNIA 90009
ATTN FRANCIS HAI
ATTN DIR, OFF OF TECH SURVIV
V. JOSEPHSON
ATTN DIR, SAT SYS DIV, GP II, V. WALL
ATTN DIR, SAT SYS DIV, GP IV, F. KELLER
ATTN LIBRARY ACQUISITION GROUP
ATTN WPNS EFF DEPT DR J REINHHEIMER
ATTN NUCLEAR + ENVIRONMENTAL STAFF
N D STOCKWELL
ATTN DR JERRY CONISAR
ATTN DIR, HARDENED REENTRY SYSTEMS,
R. MORTENSEN
ATTN J DENVENISTE

AMERICAN NUCLEONICS CORP.
ATTN SECURITY OFFICER
6036 VAREL AV.
WOODLAND HILLS, CALIFORNIA 91364
ATTN DR R N GHOSE

ARINC RESEARCH CORPORATION
WESTERN DIVISION
1222 E NORHANDY PLACE
P.O. BOX 1375
SANTA ANA, CALIFORNIA 92702
ATTN DEP MGR ENG J H ALDERMAN

ART RESEARCH CORPORATION
1100 GLENDON AVENUE
LOS ANGELES, CA. 90024
ATTN ARTHUR SANDERS
ATTN T. JORDAN

ASTRONAUTICS CORP OF AMERICA
907 SOUTH FIRST ST
MILWAUKEE WISCONSIN 53204
ATTN T KERN

AVCO SYSTEMS DIVISION
201 LOWELL STREET
WILMINGTON, MASSACHUSETTS 01887
ATTN RESEARCH LIBRARY A220, RM 2201

AVCO CORPORATION
ELECTRONICS DIVISION
2630 GLENDALE-MILFORD ROAD
CINCINNATI, OHIO 45241
ATTN RON GOLDFARB

AVCO-EVERETT RESEARCH LABORATORY
2385 REVERE BEACH PARKWAY
EVERETT MASS 02149
ATTN LOKAIN MAZZARO

BATTELLE MEMORIAL INSTITUTE
505 KING AVENUE
COLUMBUS, OHIO 43201
ATTN R.K. THATCHER
ATTN STOIAC

BEECH AIRCRAFT CORPORATION
9709 EAST CENTRAL AVENUE
WICHITA, KANSAS 67201
ATTN EDWARD L. RADELL

BELL AEROSPACE COMPANY
DIVISION OF TEXTRON, INC.
P.O. BOX 1
BUFFALO, NEW YORK 14240
ATTN MS F-11, MARTIN A. HENRY
ATTN CARL B. SCHUCH, WPNS EFFECTS GP

BELL TELEPHONE LABORATORIES, INC.
MOUNTAIN AVENUE
MURRAY HILL, NEW JERSEY 07974
ATTN H. JARRELL, RM WH-2F-153
ATTN I.G. DURAND
ATTN R.D. TAFT, RM 2B-181
ATTN A.H. CARRIER, WH-4522
ATTN H.J. BETZEL
ATTN FRANK P. ZUPA

BELL TELEPHONE LABORATORIES, INC
INTERSTATE 85 AT
MT. HOPE CHURCH ROAD
P.O. BOX 21447
GREENSBORO, NORTH CAROLINA 27420
ATTN CHARLES E. BOYLE
ATTN JAMES F. SWEENEY

BENDIX CORPORATION, THE
AEROSPACE SYSTEMS DIVISION
3300 PLYMOUTH ROAD
ANN ARBOR, MICHIGAN 48107
ATTN MR. RONALD H. PIZAREK

BENDIX CORPORATION, THE
ATTN DOCUMENT CONTROL
COMMUNICATION DIVISION
JCPPA ROAD, TOWSON
BALTIMORE, MARYLAND 21204
ATTN DOCUMENT CONTROL

BENDIX CORPORATION
RESEARCH LABORATORIES DIVISION
BENDIX CENTER
SCOUTHFIELD, MICHIGAN 48075
ATTN MANAGER, PROGRAM DEVELOPMENT,
MR. DONALD J. NIEHAUS

BENDIX CORPORATION, THE
NAVIGATION AND CONTROL DIVISION
TETERBROOK, NEW JERSEY 07608
ATTN E.E. LADEMANN
ATTN T. LAVIN, DEPT 7111
ATTN CHIEF LIBRARIAN, LYDIA FARRELL

BOEING COMPANY, THE
P O BOX 3999
SEATTLE, WASHINGTON 98124
ATTN D L OYE, 2-6005, 45-21

BOEING COMPANY, THE
P.O. BOX 3707
SEATTLE, WASHINGTON 98124
ATTN R.S. CALDWELL, MS 2R-00
ATTN H.W. WICKLEIN, MS 1F-51
ATTN A.R. LOWREY, MS 2R-00
ATTN AEROSPACE LIBRARY
ATTN B L CARLSON MS 4240

BOOZ-ALLEN APPLIED RESEARCH, INC
106 APPLE STREET
NEW SHREWSBURY, NEW JERSEY 07724
ATTN FREDERICK NEWTON

BRADDOCK, DUNN + MC DONALD, INC.
P O BOX 8885 STATION C
ALBUQUERQUE, NEW MEXICO 87108
ATTN ROBERT B. BUCHANAN

BRADDOCK, DUNN + MC DONALD, INC.
8027 LEESBURG PIKE
MC LEAN, VIRGINIA 22101
ATTN J.V. BRADDOCK
ATTN J J KALINOWSKI

BROWN ENGINEERING COMPANY, INC.
RESEARCH PARK
HUNTSVILLE, ALABAMA 35807
ATTN D. LAMBERT, MS 126

CALSPAN CORPORATION
P O BOX 235
BUFFALO, NEW YORK 14221
ATTN R H DICKHAUT, BLDG 10, RM 341.

CHRYSLER CORPORATION
DEFENSE DIVISION
P O BOX 757
DETROIT, MICHIGAN 48231
ATTN R.F. GENTILE, CIMS 435-01-21

COLLINS RADIO COMPANY
5225 C AVENUE, N. E.
CEDAR RAPIDS, IOWA 52406
ATTN E.E. ELLISON, LIBRARIAN

COMPUTER SCIENCES CORPORATION
P O BOX 530
FALLS CHURCH, VIRGINIA 22046
ATTN JOHN D ILLGEN

CUTLER HAMMER, INC.
AIL DIVISION
COMAC ROAD
DEER PARK, NEW YORK 11729
ATTN CENTRAL TECHNICAL FILES,
ARNE ANTHONY
ATTN RICHARD J MOHR

DIKWOOD CORPORATION, THE
1009 BRADBURY DRIVE, S.E.
UNIVERSITY RESEARCH PARK
ALBUQUERQUE, NEW MEXICO 87106
ATTN LLOYD WAYNE DAVIS

E-SYSTEMS INC
GREENVILLE DIVISION
MAJOR FIELD
P O BOX 1056
GREENVILLE, TEXAS 75401
ATTN LIBRARY

EFFECTS TECHNOLOGY, INC.
5303 HOLISTER AVENUE
SANTA BARBARA, CALIFORNIA 93105
ATTN EDWARD JOHN STEELE

EG&G, INC
SAN RAMON OPERATIONS
P.O. BOX 204
SAN RAMON, CALIFORNIA 94583
ATTN BARNELL G. WEST

EG&G, INC.
P.O. BOX 4339
ALBUQUERQUE, NEW MEXICO 87106
ATTN WEYLAND D. GEORGE
ATTN HILOA HOFFMAN

EMERSON ELECTRIC COMPANY
8100 FLORISSANT
ST LOUIS, MISSOURI 63136
ATTN DOCUMENT CONTROL

ENERGY CONVERSION DEVICES, INC.
1675 WEST MAPLE ROAD
TROY, MICHIGAN 48064
ATTN LIONEL ROBRINS

FAIRCHILD INDUSTRIES
SHERMAN FAIRCHILD TECHNOLOGY CENTER
FAIRCHILD DRIVE
GERMANTOWN, MARYLAND 20767
ATTN LEONARD J. SCHREIBER

FAIRCHILD CAMERA + INSTRUMENT CORP
464 ELLIS STREET
MOUNTAIN VIEW CALIFORNIA 94040
ATTN SECURITY DEPT FOR 30-204
DAVID K MYERS

GARRETT CORPORATION, THE
9851 SEPULVEDA BLVD
LOS ANGELES, CA 90009
ATTN ROBERT WEIR, DEPT 93-9

GENERAL DYNAMICS CORPORATION
CONVAIR AEROSPACE DIVISION
SAN DIEGO OPERATIONS
P.O. BOX 1950
SAN DIEGO, CALIFORNIA 92112
ATTN V J SWEENEY, INTERDIV RESEARCH

GENERAL ELECTRIC COMPANY
APOLLO + GROUND SYSTEMS, HOUSTON
1830 NASA BOULEVARD
P.O. BOX 59408
HOUSTON, TEXAS 77058
ATTN H.E. SHARP

GENERAL ELECTRIC COMPANY
P.O. BOX 1122
SYRACUSE, NEW YORK 13201
ATTN HES; BLDG 1, RM 4,
J.R. GREENBAUM
ATTN CSP 6-7; L.H. DEE

GENERAL ELECTRIC COMPANY
AEROSPACE ELECTRONICS DEPARTMENT
FRENCH ROAD
UTICA, NEW YORK 13502
ATTN W.J. PATTERSON, DROP 233
ATTN MAIL STA 624 FRED NICOTERA

GENERAL ELECTRIC COMPANY
P.O. BOX 5000
BINGHAMTON, NEW YORK 13902
ATTN B.H. SHWALTER, MD 160

GENERAL ELECTRIC COMPANY
ORDNANCE SYSTEMS
100 PLASTICS AVENUE
PITTSFIELD, MASSACHUSETTS 01201
ATTN DAVID CORMAN, MN 2276

GENERAL ELECTRIC COMPANY
100 WOODLAWN AVE
PITTSFIELD, MASSACHUSETTS 01201
ATTN FRANK FISHER, BLDG 9-209

GENERAL ELECTRIC COMPANY
RE ENTRY + ENVIRONMENTAL SYSTEMS DIVISION
P O BOX 7722
PHILADELPHIA, PENNSYLVANIA 19101
ATTN ROBERT V. BENEDICT

GENERAL ELECTRIC COMPANY
SPACE DIVISION
VALLEY FORGE SPACE CENTER
P.O. BOX 8555
PHILADELPHIA, PENNSYLVANIA 19101
ATTN JOSEPH C. PEDEY, GCF 830E
ATTN RADIATION EFFECTS LAB,
J.L. ANDREWS
ATTN LIBRARIAN, L.I. CHASEN
ATTN DANIEL EDELMAN
ATTN J.P. SPRATT, RM 9421

GENERAL ELECTRIC COMPANY
TEMP-CENTR FOR ADVANCED STUDIES
816 STATE STREET
SANTA BARBARA, CALIFORNIA 93102
ATTN DASIAE

GENERAL MOTORS CORPORATION
DELCO ELECTRONICS DIVISION
7929 SLJTH HOWELL AVENUE
OAK CREEK, WISCONSIN 53001
ATTN TECHNICAL LIBRARY 2A07,
E.T. KRUEGER

GENERAL RESEARCH CORPORATION
P.O. BOX 3587
SANTA BARBARA, CALIFORNIA 93105
ATTN TECH INFO OFFICE FOR R.D HILL

GENERAL RESEARCH CORPORATION
1501 WILSON BLVD.
ARLINGTON, VIRGINIA 22209
ATTN DR WILLIAM JOHNSON

GOODYEAR AEROSPACE CORPORATION
ARIZONA DIVISION
LITCHFIELD PARK, ARIZONA 85340
ATTN B MANNING

GRUMMAN AEROSPACE CORPORATION
SOUTH OYSTER BAY ROAD
BETHPAGE, NEW YORK 11714
ATTN J. ROGERS, PLANT 35, DEPT 535

GTE SYLVANIA, INC.
77 A STREET
NEEDHAM, MASSACHUSETTS 02194
ATTN LIR, C. THORNHILL
ATTN ELECT SYS GP S/V ENG DEPT
J A WALDRON
ATTN J H TERRELL
ATTN ELECT SYST DIV, L L BLAISDELL

GTE SYLVANIA, INC.
COMMUNICATIONS SYSTEMS DIVISION
189 B STREET
NEEDHAM, MASSACHUSETTS 02194
ATTN S/V ENG, DEPT. J.A. WALDRON
ATTN ASH DEPT E P HOTCHK
ATTN ASH DEPT DR J H TERRELL
ATTN ASH DEPT S A FIERSTON

HAZELTINE CORPORATION
PULASKI ROAD
GREEN LAWN, NEW YORK 11740
ATTN J B COLOMBO

HERCULES INCORPORATED
BACCHUS PLANT
PO BOX 98
MAGNA, UTAH 84044
ATTN 100K-26-W R WOODRUFF

HONEYWELL, INC.
AERONAUTICAL DIVISION
2600 RIDGWAY ROAD
MINNEAPOLIS, MINNESOTA 55413
ATTN RONALD R. JOHNSON, 41391
ATTN LIBRARY V BARTLETT R3679

HONEYWELL INCORPORATED
AEROSPACE DIVISION
13350 U.S. HIGHWAY 19
ST. PETERSBURG, FLORIDA 33733
ATTN MR. HARRISON H. HOBLE,
STAFF ENGINEER, MS 725-5A
ATTN ADVANCED DEVELOPMENT,
JAMES D. ALLEN 724-5
ATTN MS 725-5, R.C. SCHRADER

HONEYWELL, INC.
RADIATION CENTER
2 FORBES ROAD
LEXINGTON, MASSACHUSETTS 02173
ATTN TECHNICAL LIBRARY

HUGHES AIRCRAFT COMPANY
CENTINELA AVENUE AND TEALE STREET
CULVER CITY, CALIFORNIA 90230
ATTN R+D DIVISION,
DR. DAN BINDER (M.S. 0147)
ATTN MS 6/E110 B.W. CAMPBELL

HUGHES AIRCRAFT COMPANY
GROUND SYSTEMS GROUP
1901 WEST HALVERN AVENUE
FULLERTON, CALIFORNIA 92634
ATTN TECHNICAL LIBRARY BLDG 600 MS-C-22

INSTITUTE FOR DEFENSE ANALYSES
400 ARMY-NAVY DRIVE
ARLINGTON, VIRGINIA 22202
ATTN CLASSIFIED LIBRARY

INTELCOM/RAD TECH
P O BOX 80817
SAN DIEGO, CALIFORNIA 92138
ATTN: DR V A J VAN LINT
ATTN R L HERTZ
ATTN JAMES A NABER
ATTN LEO D COTTER
ATTN TERRY M PLANIGAN

INTERNATIONAL BUSINESS MACHINES CORP.
ROUTE 17C
OMEGO, NEW YORK 13827
ATTN D.C. SULLIVAN, DEPT M40, 102-1
ATTN FRANK FRANKOVSKY

INTERNATIONAL TELEPHONE AND TELEGRAPH
CORPORATION
492 RIVER ROAD
HUTLEY, NEW JERSEY 07110
ATTN DEFENSE-SPACE GROUP, SMTS,
FRANK JOHNSON
ATTN ALEXANDER L. RICHARDSON

KAMAN SCIENCES CORPORATION
KAMAN NUCLEAR DIVISION
1700 GARDEN OF THE GODS ROAD
COLORADO SPRINGS, COLORADO 80907
ATTN DR. ALBERT P. BRIDGES
ATTN DR. FRANK H. SHELTON
ATTN J.P. HUFFMAN
ATTN N-GAMMA LAB, DON BRYCE

LOCKHEED MISSILES AND SPACE COMPANY
3251 HANOVER STREET
PALO ALTO, CALIFORNIA 94304
ATTN DR. CLARENCE F. KODI,
DEPT. 52-11, BLDG. 204
ATTN DR LLOYD CHASE
ATTN DR M WALT, DEPT 52-10, BLDG 201
ATTN DR S E SINGER, DEPT 52-20, BLDG 20

LOCKHEED MISSILES AND SPACE COMPANY
DIVISION OF LOCKHEED AIRCRAFT CORP.
P.O. BOX 504
SUNNYVALE, CALIFORNIA 94088
ATTN H. SCHNEEMAN, 81-62
ATTN M365, DEPT 81-23, BLDG 154
ATTN L F HEARNE, D/81-14
ATTN R.W. HUNSON, DEPT 81-01, BLDG 154
ATTN W. KOZUMPLIK, TECHNICAL
INFORMATION CENTER, BLDG 201
ATTN G F HEATH D/81-14 B/154
ATTN DEPT 85-85, BLDG 154
A C FELLER
ATTN L J ROSSI D/81-62 B/150
ATTN KEVIN MC CARTHY

LTV AFRO SPACE CORPORATION
WEIGHT MISSILES + SPACE COMPANY
TEXAS DIVISION
P.O. BOX 6267
DALLAS, TEXAS 75222
ATT. TECHNICAL DATA CENTER

MARTIN MARIETTA CORPORATION
DENVER DIVISION
P.O. BOX 179
DENVER, COLORADO 80201
ATTN 6617 RESEARCH LIBRARY J R MC KEE
ATTN SPECIAL PROJECTS MAIL 0130

MARTIN MARIETTA CORPORATION
ORLANDO DIVISION
P.O. BOX 5837
ORLANDO, FLORIDA 32805
ATTN W.W. HRAS, MP-413
ATTN ENG LIBRARY, M.C. GRIFFITH, MP-30

MCDONNELL DOUGLAS CORPORATION
5301 BOLSA AVENUE
HUNTINGTON BEACH, CALIFORNIA 92647
ATTN N L ANDRADE, MS 17
8800 ADV ELECT/R+D

MCDONNELL DOUGLAS CORPORATION
P.O. BOX 516
ST. LOUIS, MISSOURI 63166
ATTN DR TOM-ENDER, DEPT 313, BLDG 33
ATTN LIBRARY

MISSION RESEARCH CORPORATION
1 PRESIDIO AVENUE
SANTA BARBARA, CALIFORNIA 93101
ATTN C.L. LONGMIRE
ATTN WILLIAM HART

MISSION RESEARCH CORP
PO BOX 1886
ALBUQUERQUE NEW MEXICO 87103
ATTN DAVID E. HEREWETHER
ATTN JAMES LONERGAN

MITRE CORPORATION, THE
ROUTE 62 AND MIDDLESEX TURNPIKE
P.O. BOX 208
BEDFORD, MASSACHUSETTS 01730
ATTN LIBRARY
ATTN M.E. FITZGERALD
ATTN THEODORE JARVIS

MOTOROLA, INC.
GOVERNMENT ELECTRONICS DIVISION
8201 EAST MC DOWELL ROAD
SCOTTSDALE, ARIZONA 85252
ATTN PHILIP L. CLAR
ATTN TECH INFO CENTER-A J KORDALEWSKI

NORTH AMERICAN ROCKWELL CORPORATION
3370 MIRALOMA AVENUE
ANAHEIM, CALIFORNIA 92803
ATTN MINUTEMAN OFC, CA 107, D C BAUSCH
ATT. J. BELL
ATTN G. MESSENGER
ATTN G MORGAN
ATTN J S MATYUCH FA70
ATTN N E AYRES
ATTN J SPETZ

NORTH AMERICAN AVIATION-COLUMBUS
NORTH AMERICAN ROCKWELL CORPORATION
4300 EAST FIFTH AVENUE
COLUMBUS, OHIO 43216
ATTN ENGINEERING DATA SERVICES,
J. ROBERTS

NORTH AMERICAN ROCKWELL CORPORATION
LOS ANGELES DIVISION
5601 WEST IMPERIAL HIGHWAY
LOS ANGELES, CALIFORNIA 90009
ATTN DONALD J STEVENS EMI/EMP+RCS
AVIONICS DESIGN
ATTN TIC BA08

NORTH AMERICAN ROCKWELL CORPORATION
SPACE DIVISION
12214 LAKEWOOD BOULEVARD
DOWNEY, CALIFORNIA 90241
ATTN TIC DEPT 096-AJ01

NORTHROP CORPORATION
NORTHROP CORPORATE LABORATORIES
3401 WEST BROADWAY
HAWTHORNE, CALIFORNIA 90250
ATTN DIR., SOLID STATE ELECTRONICS,
DR. ORLIE L. CURTIS, JR.
ATTN MR. JAMES P. RAYMOND
ATTN LIBRARY

NORTHROP CORPORATION
ELECTRONIC DIVISION
2301 WEST 120-TH STREET
HAWTHORNE, CALIFORNIA 90250
ATTN BOYCE T. AHLPORT
ATTN T6114, V R DE MARTINO

PALISADES INSTITUTE FOR
RESEARCH SERVICES, INC.
201 VARICK STREET
NEW YORK, NEW YORK 10014
ATTN RECORDS SUPERVISOR

PHILCO-FORD CORPORATION
AEROSPACE + DEFENSE SYSTEMS OPNS
AERONAUTRONIC DIVISION
FORD AND JAMBORREE ROADS
NEWPORT BEACH, CALIFORNIA 92663
ATTN DR. L. H. LINDER
ATTN E R PUNCELET JR
ATTN K C ATTINGER

PHILCO-FORD CORPORATION
WESTERN DEVELOPMENT LABORATORIES DIV.
3939 FABIAN WAY
PALO ALTO, CALIFORNIA 94303
ATTN LIBRARY
ATTN E R HAHN, MS-222
ATTN S CRAWFORD, MS-531

PULSAR ASSOCIATES, INC.
7911 HERSCHEL AVENUE
LA JOLLA, CALIFORNIA 92037
ATTN CARLETON JONES

RCA CORPORATION
GOVERNMENT AND COMMERCIAL SYSTEMS
MISSILE AND SURFACE RADAR DIVISION
MARNE HIGHWAY AND BORTON LANDING ROAD
MOORESTOWN, NEW JERSEY 08057
ATTN ELEANOR DALY

RCA CORPORATION
GOVERNMENT AND COMMERCIAL SYSTEMS
ASTRO ELECTRONICS DIVISION
P.O. BOX 800
PRINCETON, NEW JERSEY 08540
ATTN DR. GEORGE BRUCKER

RCA CORPORATION
DAVID SARNOFF RESEARCH CENTER
201 WASHINGTON ROAD
WEST WINDSOR TOWNSHIP
PRINCETON, NEW JERSEY 08540
ATTN WILLIAM J. DENWEHY

RCA CORPORATION
P.O. BOX 591
SCHERVILLE, NEW JERSEY 08876
ATTN DANIEL HAMPEL ADV COMM LAB

RCA CORPORATION
CAMDEN COMPLEX
FRONT + COOPER STREETS
CAMDEN, NEW JERSEY 08012
ATTN E. VAN KEULEN, 13-5-2

R + D ASSOCIATES
P. O. BOX 3580
SANTA MONICA, CALIFORNIA 90403
ATTN WILLIAM KARZAS
ATTN H.R. SCHAEFER
ATTN DR WM R GRAHAM
ATTN ROBERT A. POLL
ATTN S CLAY ROGERS

RADIATION INCORPORATED
P.O. BOX 37
MELBOURNE, FLORIDA 32902
ATTN JOHN H. TURNER
ATT. E V ROOS, MS 16-156

RAND CORPORATION, THE
1700 MAIN STREET
SANTA MONICA, CALIFORNIA 90406
ATTN C.M. CRAIN

RAYTHEON COMPANY
528 BOSTON POST ROAD
SUDBURY, MASSACHUSETTS 01774
ATTN HAROLD L. FLESCHEA
ATTN D.R. JONES

RESEARCH TRIANGLE INSTITUTE
P.O. BOX 12194
RESEARCH TRIANGLE PARK, NORTH CAROLINA
27709
ATTN ENG. + ENVIRON. SCIENCES DIV.,
DR. MAYRANT SIMONS, JR.

SANDERS ASSOCIATES, INC.
95 CANAL STREET
NASHUA, NEW HAMPSHIRE 03060
ATTN M L ATTEL
ATTN 1-6270, R G DESPATHY, SR PE

SANDIA LABORATORIES
ATTN DOCUMENT CONTROL
P. O. BOX 5800
ALBUQUERQUE, NEW MEXICO 87115
ATTN ORG 50, A NARATH
ATTN ORG 9353, R L PARKER
ATTN ORG 5231, C N VITTIOTE
ATTN ORG 1426, J A COOPER
ATTN TECHNICAL LIBRARY
ATTN ORG 1935, J.E. GOVER
ATTN J D APPEL
ATTN J W KANE

SANDIA LABORATORIES
LIVERMORE LABORATORY
ATTN DOCUMENT CONTROL
P.O. BOX 969
LIVERMORE, CALIFORNIA 94550
ATTN T.A. DELLIN
ATTN K A MITCHELL, 8157
ATTN G OTEY 8178
ATTN J L WIRTH 8340
ATTN SUPERVISOR, LIBRARY DIV
ATTN J A MOGFORD DIV 8341

SCIENCE APPLICATIONS INC
HUNTSVILLE DIVISION
2109 W CLINTON AVE
SUITE 700
HUNTSVILLE ALABAMA 35805
ATTN N R BYEN

SINGER-GENERAL PRECISION, INC
1150 MC BRIDE AVENUE
LITTLE FALLS, NEW JERSEY 07424
ATTN ABRAHAM WITTELES, RADIATION
EFFECTS SUPERVISOR, 3-5820

SPERRY RAND CORPORATION
SPERRY GYROSCOPE DIVISION
GREAT NECK, NEW YORK 11020
ATTN PAUL HARRAFFIN, DEPT 4282

SPERRY RAND CORPORATION
UNIVAC DIVISION
DEFENSE SYSTEMS DIVISION
P.O. BOX 3525, MAIL STATION 1931
ST. PAUL, MINNESOTA 55101
ATTN DENNIS AMUNDSON, MS 5261
ATTN J.A. INDA, MS 5451
ATTN A BROWN, MS 8931

SPERRY RAND CORPORATION
SPERRY FLIGHT SYSTEMS DIVISION
P O BOX 2592
PHOENIX, ARIZONA 85002
ATTN PAT DEVILLIER
ATTN D A SCHOW, RM 104C

STANFORD RESEARCH INSTITUTE
333 RAVENSWOOD AVENUE
MENLO PARK, CALIFORNIA 94025
ATTN MR. PHILLIP DOLAN
ATTN MR. ARTHUR LEE WHITSON
ATTN DR. ROBERT A. ARMISTEAD
ATTN J.A. BAER, J1015

STANFORD RESEARCH INSTITUTE
306 WYNN DRIVE, N.W.
HUNTSVILLE, ALABAMA 35805
ATTN SR RES ENG, M. MORGAN
ATTN HAROLD CAREY
ATTN WILLIAM DRUEN

SUNDSTRAND AVIATION
4747 HARRISON AVENUE
ROCKFORD, ILLINOIS 61101
ATTN DEPT 7635W, CURT WHITE

SYSTEMS, SCIENCE AND SOFTWARE, INC.
P.O. BOX 1620
LA JOLLA, CALIFORNIA 92037
ATTN GLEN SEAY

SYSTRON-DONNER CORPORATION
200 SAN MIGUEL ROAD
CINCINNATI, CALIFORNIA 94520
ATTN HAROLO D. MORRIS

TEXAS INSTRUMENTS, INC.
P.O. BOX 5474
DALLAS, TEXAS 75222
ATTN R + D PROJECT MANAGER,
MR DONALD J. MANUS, MS 72
ATTN RADIATION EFFECTS PROGRAM MGR.,
MR. GARY F. HANSON

TRW SYSTEMS GROUP
ONE SPACE PARK
REDDING BEACH, CALIFORNIA 90278
ATTN MR. R. KINGSLAND
ATTN MR. D. JORTNER
ATTN MR. A. ANDERMAN
ATTN B. SUSSHOLTZ
ATTN TECH INFO CENTER/S-1930
ATTN LILLIAN SINGLETARY R1/2154
ATTN DR. W.A. ROBINSON, R1/2028
ATTN R M WHITNER
ATTN R MOLMUD
ATTN JAMES GORDON

TRW SYSTEMS GROUP
SAN BERNARDINO OPERATIONS
P.O. BOX 1310
SAN BERNARDINO, CALIFORNIA 92402
ATTN J.M. GORMAN, MGR, WPN SYS ENG
ATTN D W PUGSLEY
ATTN E W ALLEN
ATTN H S JENSEN
ATTN J E DAHNKE
ATTN R H KARCHER, MS 526/712

UNITED AIRCRAFT CORPORATION
HAMILTON STANDARD
BRADLEY INTERNATIONAL AIRPORT
WINDSOR LOCKS, CONNECTICUT 06369
ATTN RAYMOND G GIGUERE

UNITED AIRCRAFT CORPORATION
NORDEN DIVISION
HELEN STRELT
NORWALP, CONNECTICUT 06051
ATTN CONRAD CORDA

WESTINGHOUSE ELECTRIC CORPORATION
DEFENSE AND SPACE CENTER
DEFENSE AND ELECTRONIC SYSTEMS CENTER
P.O. BOX 1693
BALTIMORE, MARYLAND 21203
ATTN HENRY P KALAPACA, MS 3519

WESTINGHOUSE ELECTRIC CORPORATION
RESEARCH AND DEVELOPMENT CENTER
1310 BEULAH ROAD (CHURCHILL BDR)
PITTSBURGH, PENNSYLVANIA 15235
ATTN WILLIAM E. NEWLL

WESTINGHOUSE ELECTRIC CORPORATION
ASTRONUCLEAR LABORATORY
P O BOX 1084
PITTSBURGH, PENNSYLVANIA 15236
ATTN P.W. DICKSON

HARRY DIAMOND LABORATORIES
ATTN EINSEL, DAVID W., COL. COMMANDING
OFFICER/CARTER, W.W./GUARINO, P.A.
KALMUS, H.P./SOMMER, H.
ATTN HOKTON, B.M., TECHNICAL DIRECTOR
WILLIS, B.F.
ATTN APSTEIN, M., 002
ATTN CHIEF, 0021
ATTN CHIEF, 0026
ATTN CHIEF, LAB 100
ATTN CHIEF, LAB 200
ATTN CHIEF, LAB 300
ATTN CHIEF, LAB 400
ATTN CHIEF, LAB 500
ATTN CHIEF, LAB 600
ATTN CHIEF, DIV 700
ATTN CHIEF, DIV 800
ATTN CHIEF, LAB 900
ATTN CHIEF, LAB 1000
ATTN CHIEF, 041
ATTN HOL LIBRARY 4 COPIES
ATTN CHAIRMAN, EDITORIAL COMMITTEE 4 COPIES
ATTN CHIEF, 047
ATTN TECH REPORTS, 013
ATTN PATENT LAW BRANCH, 071
ATTN CHIEF, 0024
ATTN S MARCUS, 0024
ATTN TOMPKINS, J E, 270
ATTN CHIEF, 280
ATTN MILETTA, J.R., 1010
ATTN CHIEF, 1020
ATTN R WONG 1020
ATTN CHIEF, 1030
ATTN W I WYATT, JR, 1000
ATTN ADAM F RENNEN 1000
ATTN J HEILFUSS WRF
ATTN JOHN BOMBARDI WRF
ATTN ROBERT GRAY WRF
ATTN JAVIS KLEBERS WRF
ATTN LEO LEVITT WRF
ATTN GEORGE MEKEL WRF
ATTN JOHN ROSADO 1W15 92 270 20 COPIES

UNCLASSIFIED

Security Classification

DOCUMENT CONTROL DATA - R & D		
<i>(Security classification of title, body of abstract and indexing annotation must be entered when the overall report is classified)</i>		
1. ORIGINATING ACTIVITY (Corporate author) Harry Diamond Laboratories Washington, D.C. 20438		2a. REPORT SECURITY CLASSIFICATION Unclassified
		2b. GROUP
3. REPORT TITLE SIMULATION OF A SIMPLE LORENTZ PLASMA WITH A RANDOM DISTRIBUTION OF INDUCTIVELY LOADED DIPOLES		
4. DESCRIPTIVE NOTES (Type of report and inclusive dates) Technical Report		
5. AUTHOR(S) (First name, middle initial, last name) George Merkel		
6. REPORT DATE November 1973	7a. TOTAL NO. OF PAGES 54	7b. NO. OF REFS 26
8a. CONTRACT OR GRANT NO.		9a. ORIGINATOR'S REPORT NUMBER(S) HDL-TR-1637
b. PROJECT NO. DNA Subtask R99QAXEB088 Work Unit 04 MIPR-73-589		9b. OTHER REPORT NO(S) (Any other numbers that may be assigned this report)
c. AMCMS Code: 691000.22.63516		
d. HDL Proj: E053E3		
10. DISTRIBUTION STATEMENT Approved for public release; distribution unlimited		
11. SUPPLEMENTARY NOTES		12. SPONSORING MILITARY ACTIVITY Defense Nuclear Agency Work Unit Title "Source-Region Coupling"
13. ABSTRACT <p>The feasibility of simulating a simple Lorentz plasma with an artificial dielectric constructed from a random distribution of inductively loaded dipoles is investigated. Both the differences and similarities between the macroscopic electromagnetic properties of the artificial dielectric and a Lorentz plasma are discussed.</p>		

DD FORM 1473

NOV 68

REPLACES DD FORM 1473, 1 JAN 64, WHICH IS OBSOLETE FOR ARMY USE.

UNCLASSIFIED

Security Classification

53

UNCLASSIFIED

Security Classification

14. KEY WORDS	LINK A		LINK B		LINK C	
	ROLE	WT	ROLE	WT	ROLE	WT
Nuclear Electromagnetic Pulse						
Plasma Simulation						
Artificial Dielectric						
Ionized Air						
Inductively Loaded Dipoles						

UNCLASSIFIED

Security Classification